Report for Year 5 (April 2016-September 2017) of the Induced Seismicity Monitoring Project (ISMP)

Alireza Babaie Mahani, Project Seismologist

February 2018

Contents

Contents 2
Executive Summary 3
Update on the Performance of the Seismographic Network 5
Ground Motion Database 14
Seismicity in 2016-2017 21
Fluid Injection and Induced Seismicity 23
Communication and Extension Plan 26
  Presentations 26
  Technical Papers 29
Current Research 31
  Reconstruction of clipped waveforms 31
Conclusions 33
Acknowledgement 34
References 34
Appendix A: Earthquakes between January 2016 and October 2017 37
Appendix B: Yukon Geological Survey Performance Report 52

Executive Summary

The BC Seismic Research Consortium was established in 2012 to monitor oil and gas activities across northeast British Columbia (NE BC) and its connection to induced seismicity in the region. As a result, eight seismographic stations were installed between 2013 and 2014 to enhance the capability of the seismographic network which only relied on two broadband stations before then. Two more stations were also added to the network in 2015 and 2016; a new station was installed in Rainbow Lake, Alberta and another station was purchased from Canadian Natural Resources Limited in the Graham area of the Montney Play. The cost of these stations and their maintenance is shared 50/50 between Geoscience BC and the BC Oil and Gas Research and Innovation Society (BC OGRIS). Technical and financial support is provided by the BC Oil and Gas Commission, Canadian Association of Petroleum Producers, and the Sidney office of the Geological Survey of Canada. In 2016, through collaboration with the Yukon Geological Survey, five new stations were installed in the Liard Basin which has significantly increased the monitoring capability of the network in this area. Through another collaboration with the McGill University, eight stations were installed in an area to the south of Fort St. John and north of Dawson Creek in the summer of 2017 for the purpose of detailed analysis of induced seismicity in this region. Overall, the magnitude of completeness across NE BC is ~2; an improvement of 1 magnitude unit compared to the era before 2013. Moreover, the minimum detectable magnitude can be ~0.4 meaning that detailed analysis of geological structures responsible for induced events is now possible in NE BC. The improved seismic network also results in much better solutions for the location of small earthquakes across NE BC making it possible to more accurately relate induced earthquakes with injection operations. In this report, an update on the evaluation of the performance of the current network is presented through analysis of the

minimum detectable magnitude and epicentral uncertainty of the events across NE BC. Some of the results on the analysis of ground motion amplitudes compiled through collaboration with industry are also presented which is then followed by an overview of seismicity across NE BC in 2016-2017 and a case study on the relation between fluid injection and seismic activity in northern Montney Play. Throughout the 2016-2017 the members of the BC Seismic Research Consortium have presented their work in conferences and journal publications. A list of these presentations and papers is given in this report. Finally, current research topics are discussed. The two appendices at the end of this report include the earthquake catalogue for the period January 2016 and September 2017 and the Performance of the Yukon Geological Survey seismographic stations in the Liard Basin.

Update on the Performance of the Seismographic Network

Since the installation of seismographic stations in northeast British Columbia (NE BC) in 2013 as the mandate of the BC Seismic Research Consortium (Salas, et al., 2013, Salas and Walker, 2014), the ability to monitor small earthquakes from oil and gas activities has improved significantly. Babaie Mahani et al. (2016) evaluated the performance of the seismographic network in NE BC by analyzing the magnitude of completeness and minimum detectable magnitude across the region. Using the earthquake catalogue of Natural Resources Canada (NRCan), magnitude of completeness was calculated for three periods of 1985-2002, 2003-2013, and 2013-2015 (Figure 1). While magnitude of completeness for the first two periods for which there were only two permanent broadband stations in NE BC (stations FNBB and BMBC in Figure 2) was ~3, it has decreased by ~1 unit of magnitude since the installation of seismographic stations in 2013. Figure 2 shows the minimum detectable magnitude across NE BC based on the level of ambient noise at each seismographic station and estimation of peak ground velocity (PGV) through simulation of ground motion amplitudes. Overall, the theoretical minimum detectable magnitude for NE BC using the seismographic stations shown in Figure 2, is below 2.6 and it can be as low as 1.6 for areas of the Montney Play and Horn River Basin that are well covered by the regional network (Babaie Mahani et al., 2016). Such a conclusion is consistent with the results obtained from analysis of NRCan earthquake catalogue showing a magnitude of completeness of ~2 for the period 2013–2015 (Figure 1). In contrast, the minimum detectable magnitude for most areas across NE BC was ~2.8-3.0 before 2013 (Schultz et al., 2015; Salas 2016). With the addition of new seismographic stations since 2015, the performance of the seismographic network shows significant improvement in the minimum detectable magnitude and epicentral uncertainty across the region. Figure 3 shows the current distribution of

seismographic stations in NE BC and surrounding areas that are used in the routine earthquake location by NRCan.

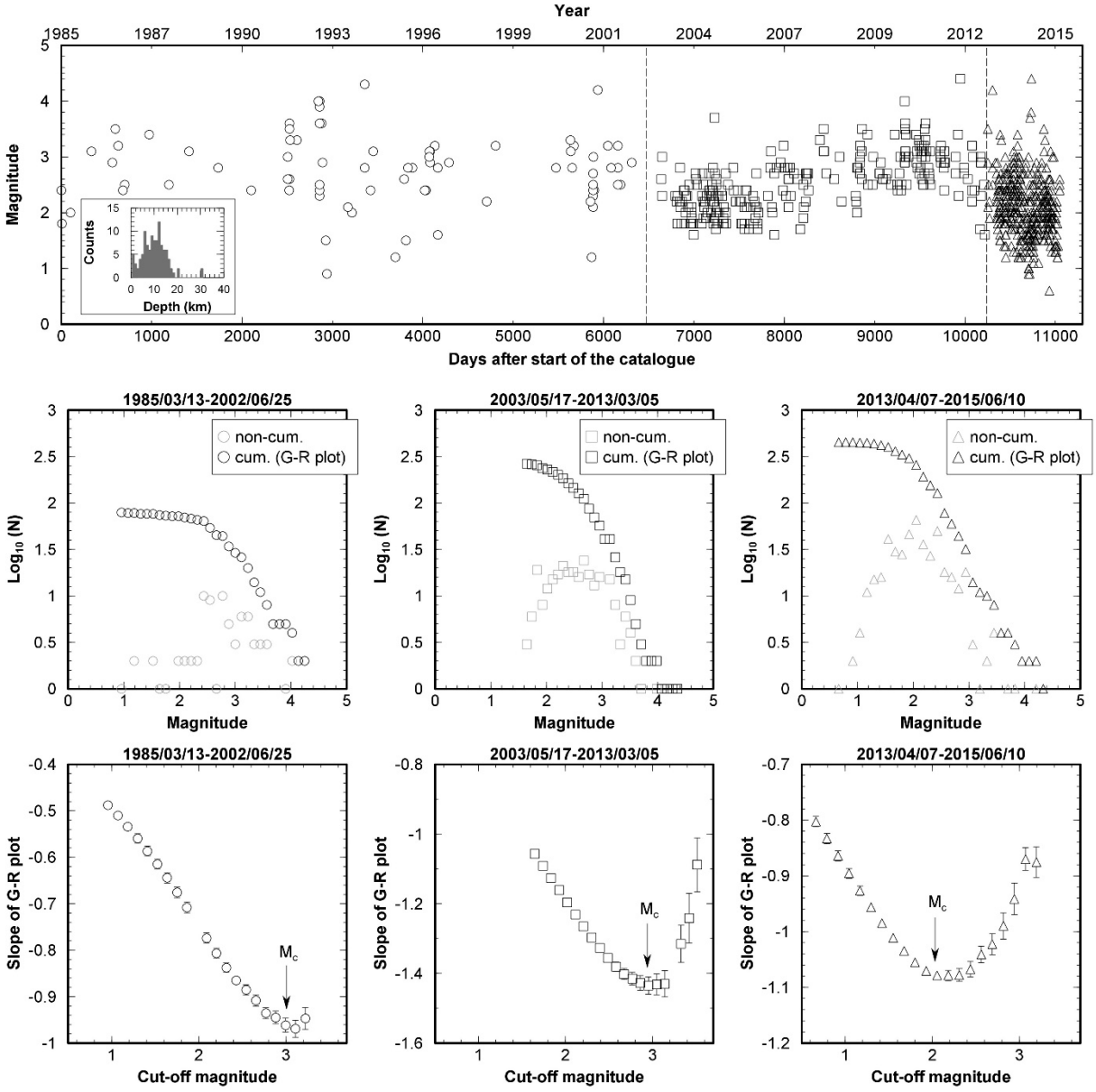

Figure 1. (top) The temporal distribution of seismicity in northeast British Columbia from 1985 to 2015 plotted with different symbols. The inset diagram is the histogram of the reported depths in the catalogue after fixed values were excluded. The dashed lines mark the three corresponding time periods in the middle and bottom plots. (middle) Cumulative (Gutenberg–Richter plot) and noncumulative frequency–magnitude distributions for each episode of seismicity. (bottom) variation of the slope of Gutenberg–Richter plot with cut-off magnitude. Note the decrease in the magnitude of completeness (M_c) from ~3 in the first and second periods to ~2 in the third period. From Babaie Mahani et al. (2016).

In Figure 3 seismographic stations from four networks are shown; the Canadian National Seismic Network (CNSN); the Regional Alberta Observatory for Earthquake Studies Network, the Yukon Northwest Seismic Network, and the Yukon Geological Survey Seismic Network. Figure 4 shows the updated minimum detectable magnitude across NE BC (gridded area in Figure 3) using all the stations shown in Figure 3. The improved minimum detectable magnitude is between 1.4 to 2.4 showing 0.2 unit of magnitude reduction in detectable magnitudes compared to the previous study (Figure 2).

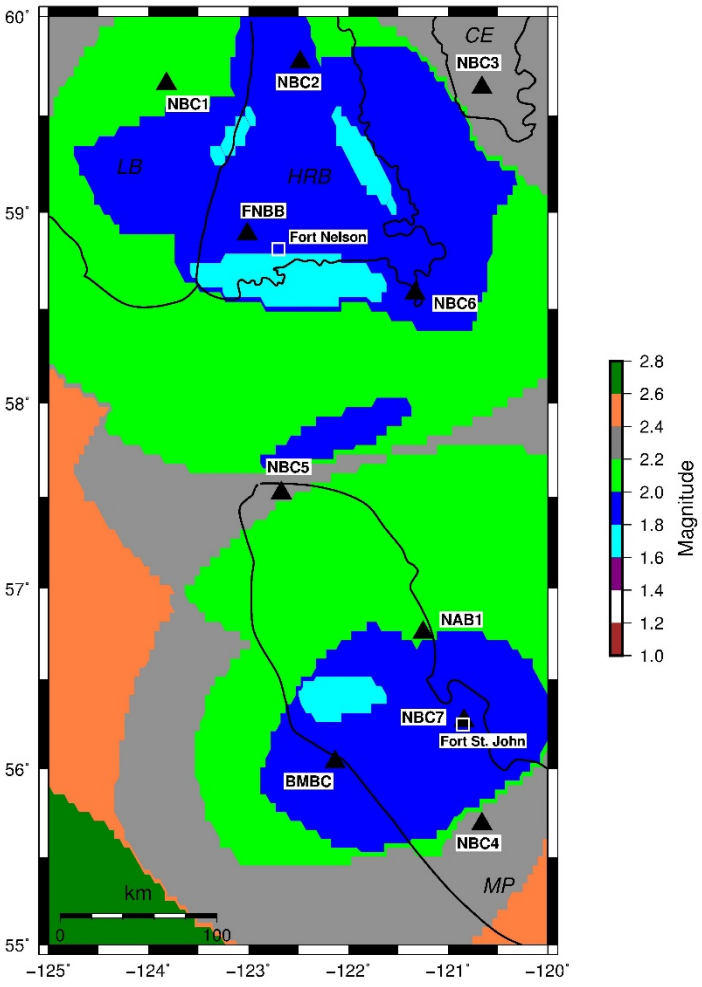

Figure 2. Minimum detectable magnitude across northeast British Columbia. Black triangles are the seismographic stations of the Canadian National Seismic Network. From Babaie Mahani et al. (2016).

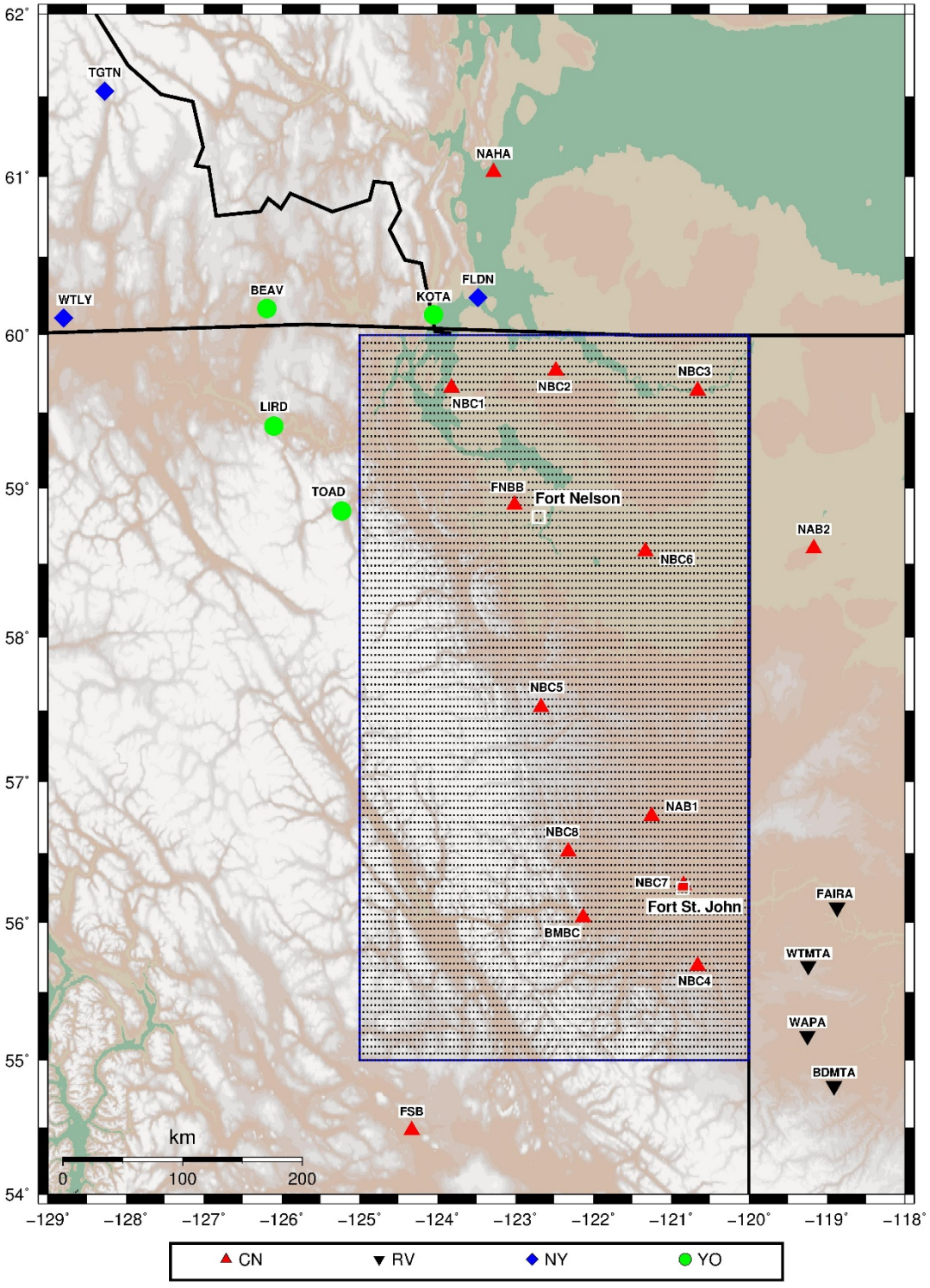

Figure 3. Distribution of the current seismographic stations. The gridded area marks the same region as in Figure 2. CN is the Canadian National Seismic Network, RV is the Regional Alberta Observatory for Earthquake Studies Network, NY is the Yukon Northwest Seismic Network, YO is the Yukon Geological Survey Seismic Network.

Moreover, with the addition of new stations, the minimum detectable magnitude extends to larger areas. For example, note that the magnitude 1.6 which covered only small regions in the northern Montney Play (Figure 2) now extends to larger areas (Figure 4).

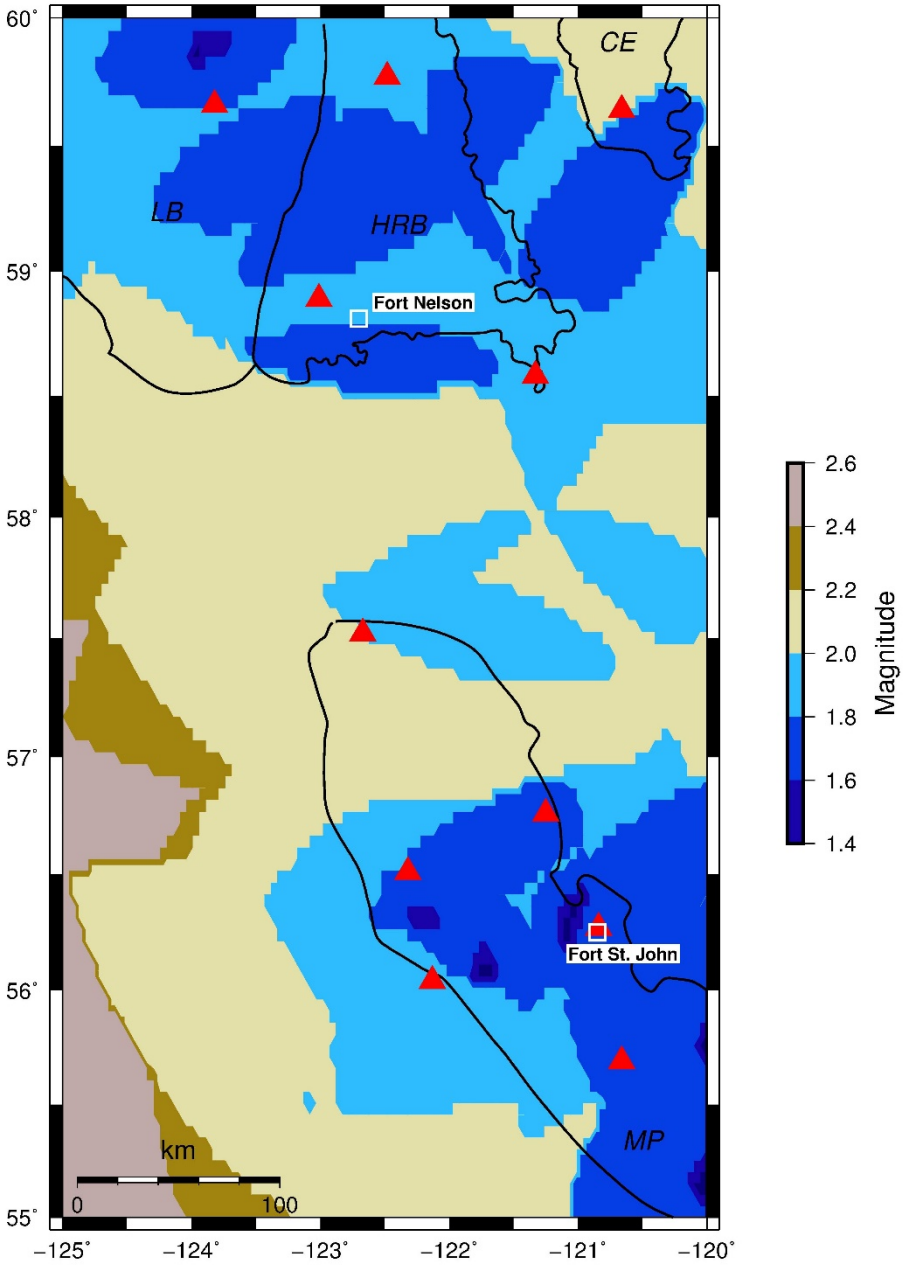

Figure 4. Minimum detectable magnitude across northeast British Columbia using all the stations shown in Figure 3. Red triangles are the seismographic stations of the Canadian National Seismic Network.

The uncertainty in the location of an event is usually shown by error ellipses which represent the shape and orientation of the error axes (semi-major and semi-minor axes of the error ellipse). Here, the square root of the sum of semi-major and semi-minor error axes was used to calculate the uncertainty shown in Figure 5. The total epicentral uncertainty for events with magnitude 2.0 in areas well covered by the seismographic stations is below 3.5 km.

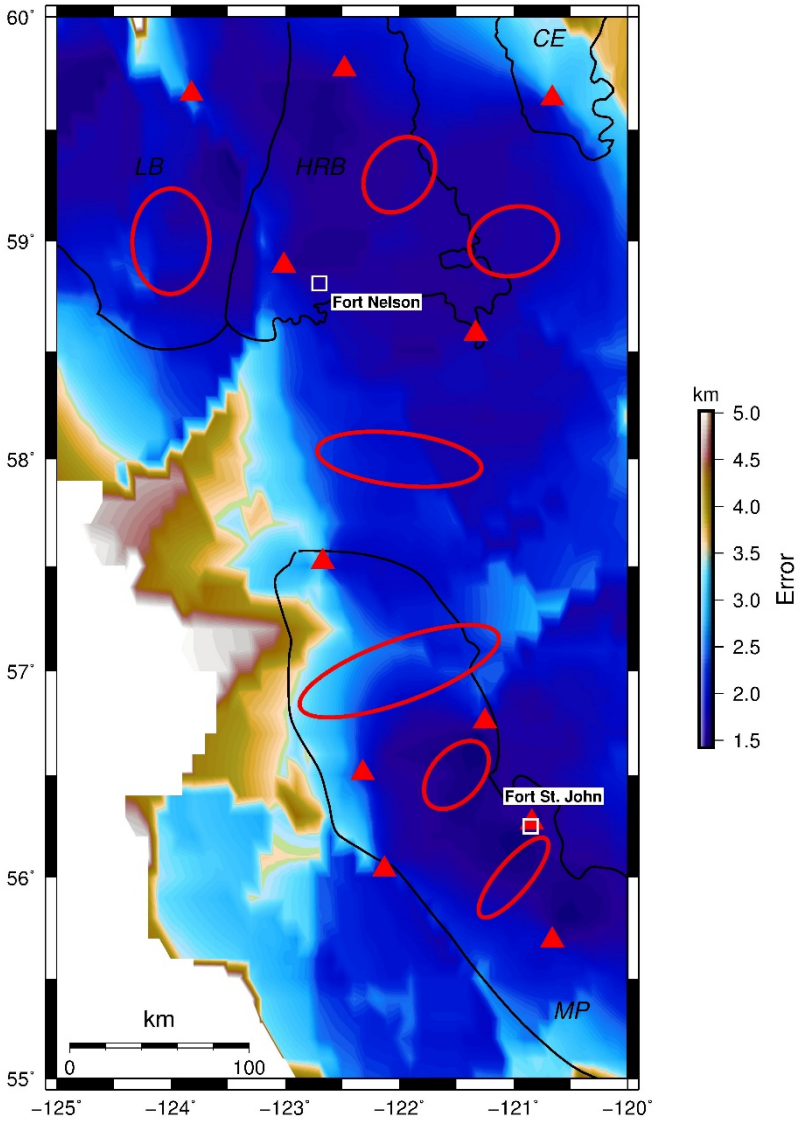

Figure 5. Total uncertainty in the epicentral location for events with magnitude 2.0 across northeast British Columbia using the stations shown in Figure 3. The ellipses show the orientation of the semi-major and semi-minor axes of uncertainty at some locations. Red triangles are the seismographic stations of the Canadian National Seismic Network.

In contrast, the total epicentral uncertainty for the same region was higher even for larger events (e.g. ~7 km for an M 3.0 event) before 2013 (Schultz et al., 2015). The red ellipses show the shape and orientation of the error axes in some locations. The orientation of semi-major and semi-minor axes mainly depends on the geometry of the seismographic network. In NE BC, the error in the longitudinal direction can be higher than the one in the latitudinal direction, specifically in the northern Montney Play (Figure 5). To better see this, Figures 6 and 7 show the semi-major (longitudinal) and semi-minor (latitudinal) axes of error, respectively.

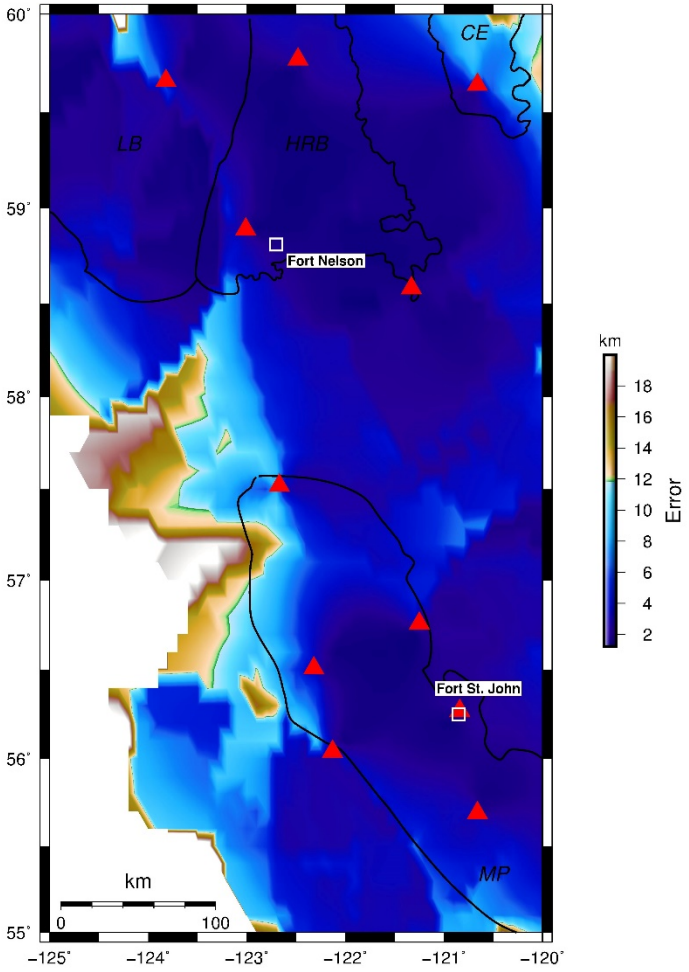

Figure 6. Semi-major (longitudinal) axis of epicentral uncertainty for events with magnitude 2.0 across northeast British Columbia. Red triangles are the seismographic stations of the Canadian National Seismic Network.

For example, the error in the longitudinal (east-west) direction for areas in the northern Montney play (the east-west elongated red ellipse in Figure 5) can be as large as 6-8 km (Figure 6) while the error in the latitudinal (north-south) direction can be ~1.5 km (Figure 7).

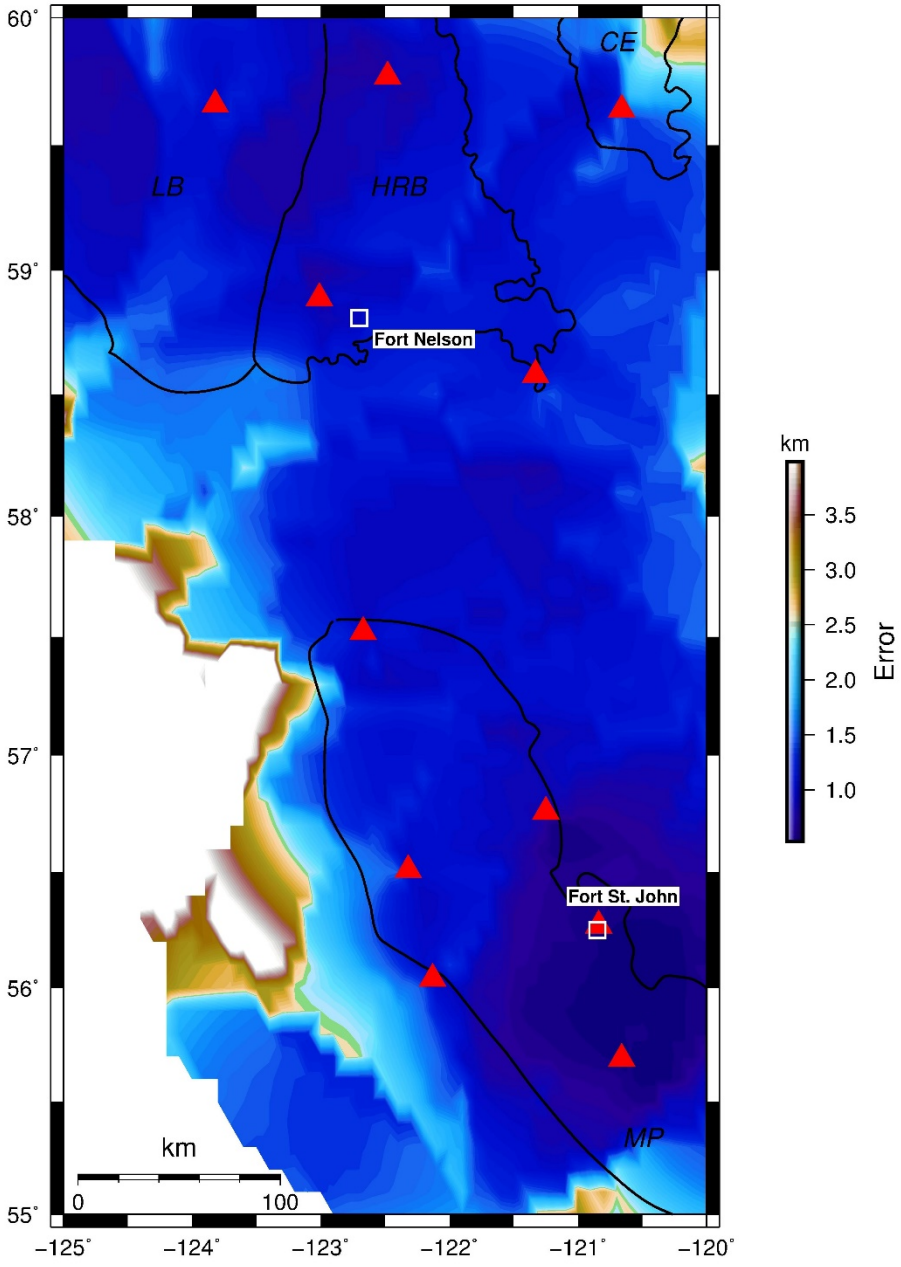

Figure 7. Semi-minor (latitudinal) axis of epicentral uncertainty for events with magnitude 2.0 across northeast British Columbia. Red triangles are the seismographic stations of the Canadian National Seismic Network.

Recently through a collaboration with the McGill University, 8 broadband seismographic stations have been installed in the summer of 2017 in the area south of Fort St. John and north of Dawson Creek. This new addition of stations will significantly improve the ability of the seismographic network in detection of small induced events and provide valuable data for seismological studies. Figure 8 shows the theoretical minimum detectable magnitude as the result of these new stations. The minimum detectable magnitude can be reduced by up to 1 unit of magnitude from 1.4 (Figure 4) to 0.4 (Figure 8) for regions around Fort St. John and Dawson Creek.

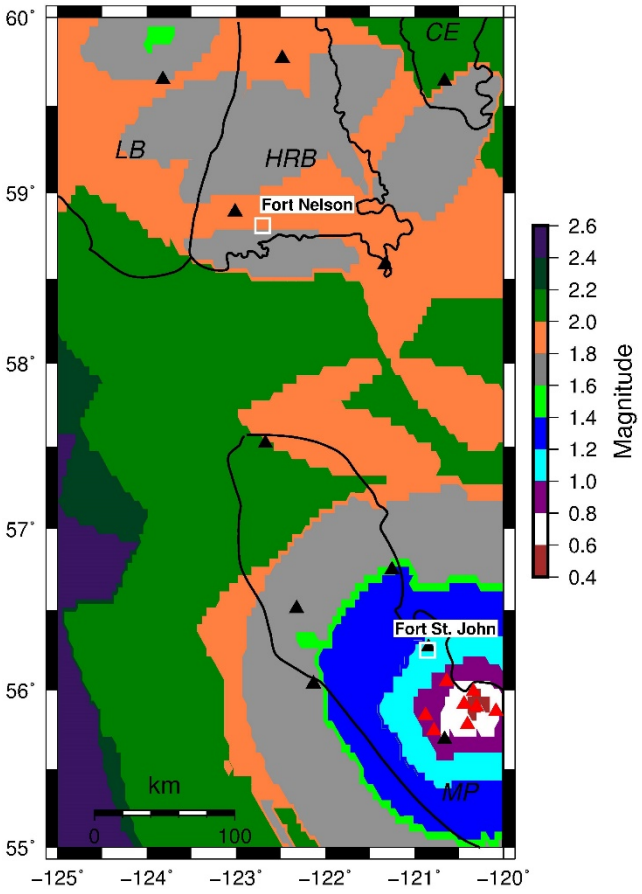

Figure 8. Theoretical minimum detectable magnitude across northeast British Columbia after the addition of McGill seismographic stations in south of Fort St. John. Red triangles show the location of the McGill stations while the black triangles show the location of the Canadian National Seismic Network stations.

Ground Motion Database

One of the major issues regarding shallow induced earthquakes is the ground motion amplitudes. Although, most induced events in NE BC have small magnitudes (< 3), shallow depth of these events can be a controlling factor in the observation of large ground motion amplitudes that can be concerning to the public and infrastructures such as the BC Hydro Site C project. For this reason, the BC Oil and Gas Commission has taken an initiative in characterization of ground motion amplitude across the Montney Play. Companies are required to install accelerometers in areas with previous known induced seismicity and submit data if ground motions in excess of 0.02 g are recorded by their stations. As of June 1, 2016, companies are required to provide waveform data in the SEED (the Standard for the Exchange of Earthquake Data) format suitable for ground motion analysis along with reports of ground motion values including peak ground acceleration (PGA) and response spectral acceleration (PSA). These reports and waveforms would provide valuable data for the analysis of ground motion amplitudes at distances close to the source, where public datasets are usually sparse. Using data provided by industry, Babaie Mahani and Kao (2018) analyzed ground motion amplitudes from small earthquakes in NE BC at hypocentral distance < 45 km. Figure 9 shows the distribution of earthquakes and seismographic stations used in their study. Waveforms from 219 local events were used, of which 129 events occurred in the Graham area and 90 events in the Septimus area (Figure 9). For the Graham area, the Canadian Natural Resources Limited (CNRL) network recorded 123 events during the time period between 21 March 2014 and 28 August 2015, whereas the Canbriam Energy network recorded 2 events on 1 May and 11 June 2016. There were also four events recorded by CNSN station 1 (NBC8 in Figure 3) on 30 December 2016, 19 and 21 April 2017, and 8 June 2017. For the Septimus area, the CNRL network recorded 81 events during the time period between 16

April 2014 and 12 October 2014. The Arc Resources network recorded four events on 14 and 16 January 2017, and 10 June 2017, whereas the Encana seismographic station recorded five events during the time period between 15 and 29 July 2017. Data from Arc Resources also includes waveforms from the two CNSN stations 1 and 19 (NBC7 and NBC4 in Figure 3) in the Septimus area.

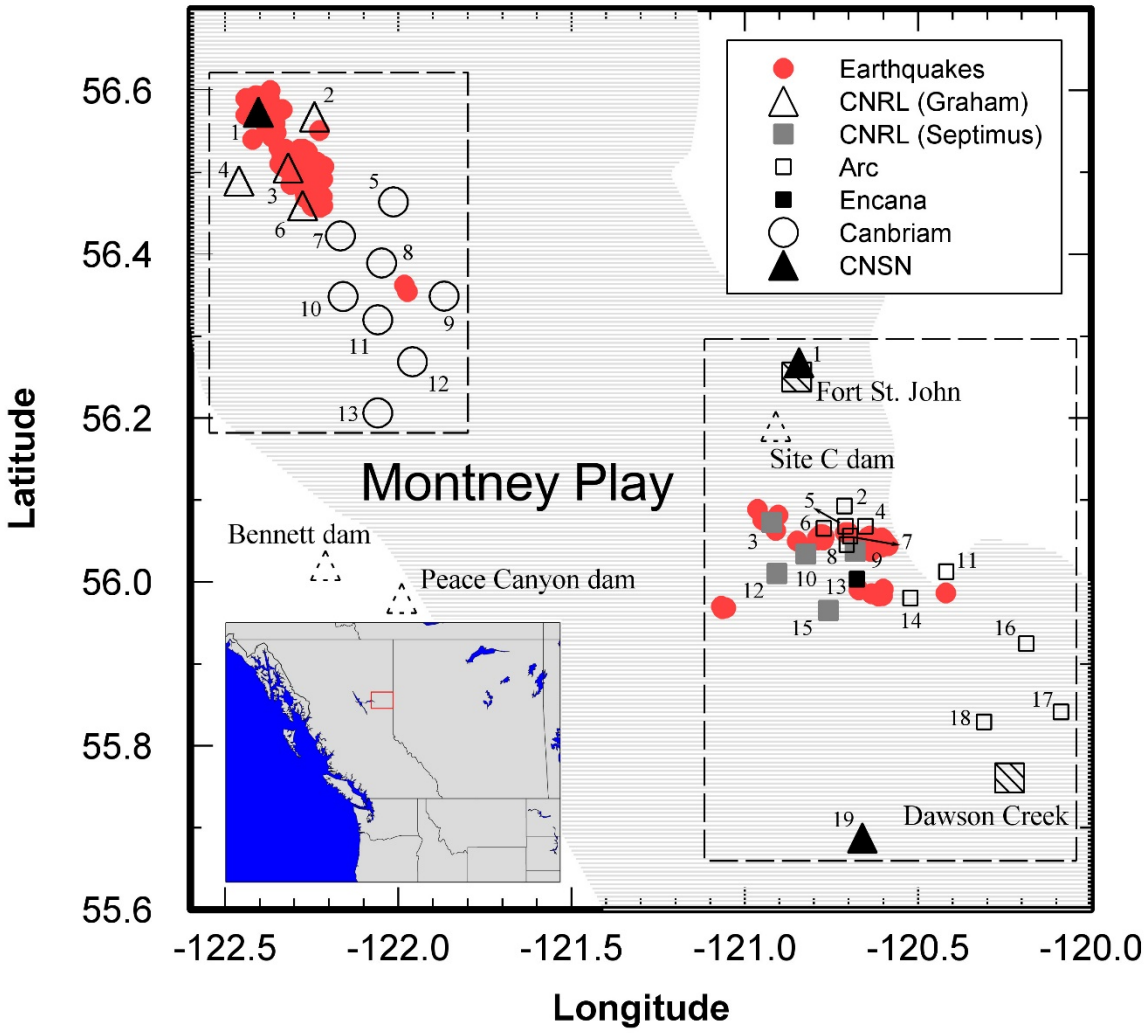

Figure 9. Map of the Montney Play of northeast British Columbia and distribution of the earthquakes and stations. Boxes show the Graham and Septimus areas with local seismograph stations numbered in each area. Triangles with dashed outlines mark the approximate locations of BC Hydro dams. The inset shows the location of the study area on the national map. CNRL, Canadian Natural Resources Limited; CNSN, Canadian National Seismic Network. From Babaie Mahani and Kao (2018).

The effect of local geological materials or the site condition on ground motion amplitudes is as important as (if not more) parameters of the source (e.g. magnitude) and path (e.g. quality factor). The horizontal-to-vertical (H/V) spectral ratio of ground motion is often used to estimate site amplification and site fundamental frequency (e.g. Nakamura 1989). Figure 10 shows the average of the logarithm values of H/V spectral ratios of ground motion (referred as the log-averaged ratio) for each station in the Graham and Septimus areas as a function of frequency. Overall, stations in the Septimus area show larger variability in the H/V ratios than those in the Graham area. The range of the maximum H/V ratios (peak values in Figure 10) is 1.6–12.6 (0.2–1.1 in log unit) and 2.5–7.9 (0.4–0.9 in log unit) for the Septimus and Graham areas, respectively (Babaie Mahani and Kao, 2018).

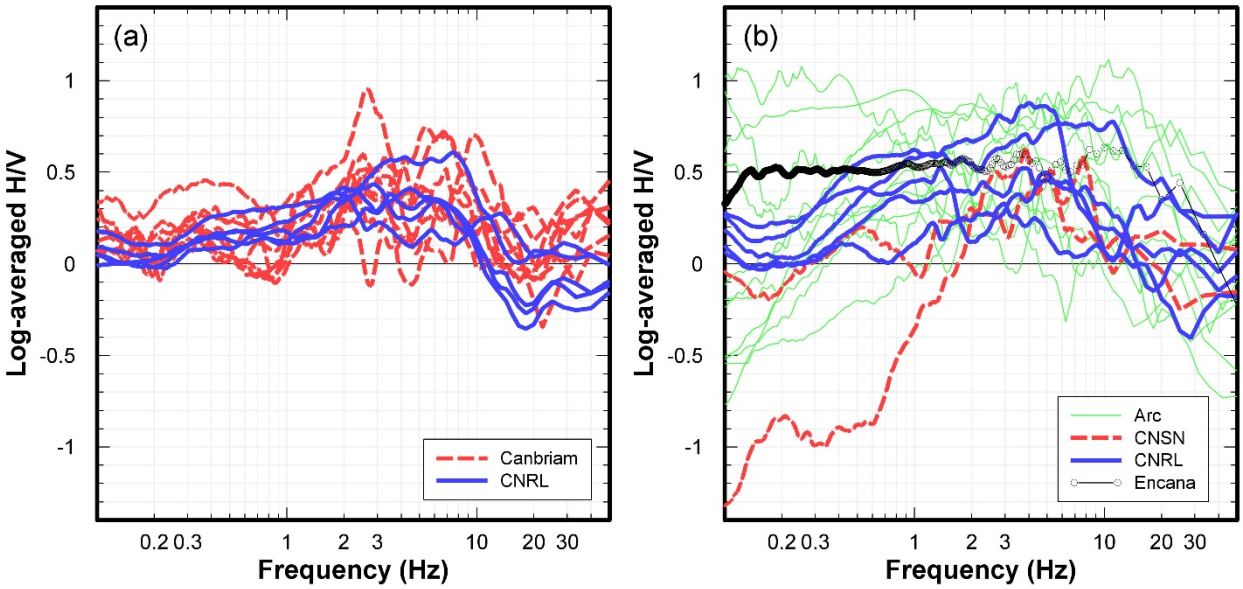

Figure 10. Log-averaged spectral ratio of horizontal-to-vertical (H/V) component of ground motion versus frequency for the seismograph stations in the (a) Graham and (b) Septimus areas. From Babaie Mahani and Kao (2018).

Figure 11 shows the geometric mean of the horizontal components for PGA and PGV corrected to the reference site condition B/C (shear-wave velocity in the top 30 m of soil column, Vs_{30} = 760 m/sec) versus hypocentral distance. Also plotted in Figure 11, are the attenuation models obtained for the two areas of Graham and Septimus in NE BC for different magnitudes (Babaie Mahani and Kao, 2018).

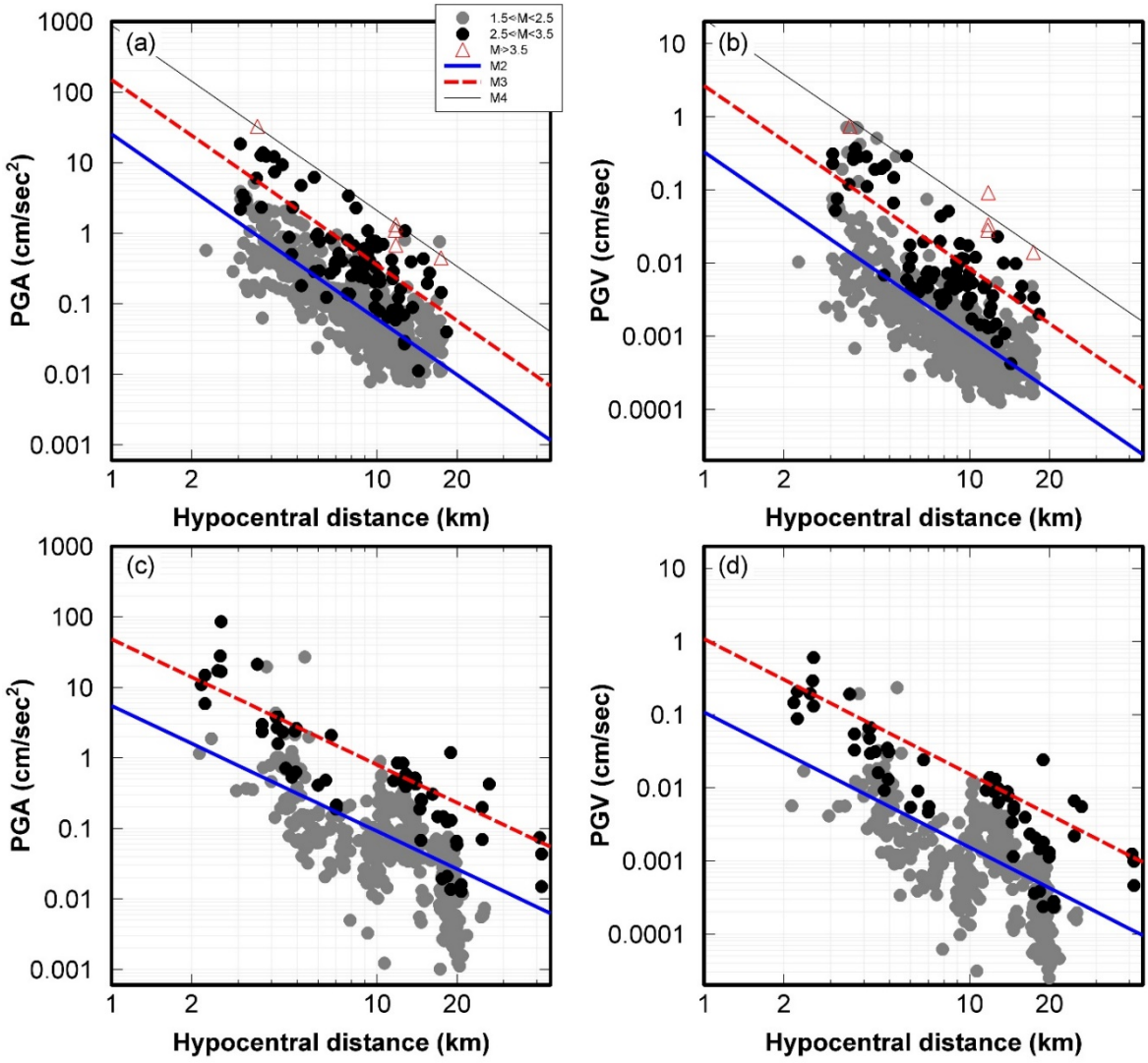

Figure 11. Geometric mean of the horizontal components of motion corrected for the reference site condition (shear-wave velocity in the top 30 m; Vs_{30} = 760 m/sec) for peak ground acceleration (PGA) and peak ground velocity (PGV) for different magnitude bins in the Graham (a and b) and Septimus (c and d). Also plotted are the prediction models obtained for the two areas. From Babaie Mahani and Kao (2018).

Although the assessment of ground motion amplitudes (PGA, PGV, and PSA) is useful in understanding the potential seismic hazard to nearby structures, duration of the strong ground motion can also be important. For example, at strong ground accelerations beyond the elastic threshold of materials, permanent deformation, or breakage can be exacerbated by a relatively long wavetrain. Numerous definitions of strong motion duration have been suggested by researchers in the past. Bommer and Martinez-Pereira (1999) reviewed some 30 definitions of duration and classified them into generic groups. The bracketed duration (Db) is defined as the time frame for which the ground motion is above a prescribed threshold (e.g., 50 cm/sce^2). The significant duration (Ds) is based on the mean-square integral of amplitude which is related to the seismic energy content of the ground motion (Trifunac and Brady, 1975). The Arias intensity (Arias, 1970) calculates the energy content as

$$AI = \frac{\pi}{2g}\int_0^t a^2\,(\tau)d\tau \qquad (1$$

in which $a(\tau)$ is the acceleration time history, t is the total duration of the accelerogram, and g is the acceleration due to Earth's gravity. Figure 12 describes the two definitions of significant and bracketed duration. In Figure 12a, the east–west component waveform from an M 3.0 event recorded at one of the Arc seismographic stations at hypocentral distance of ~2.6 km with the PGA of ~115 cm/sec^2 is shown. The normalized Arias intensity of the waveform is also plotted. Intensity increases gradually from the onset of P wave at ~21.5 sec, followed by a significant change in the slope with the arrival of the S wave at ~21.9 sec. The strongest ground motion is observed at ~22.2 sec, corresponding to a sharp increase in the intensity and most likely due to the arrival of surface waves (Figure 12a). After this sharp increase, intensity gradually increases to its maximum value. Using Equation (1), Ds can be determined as the time frame

corresponding to the strong motion part of the waveform. Using the 5% and 95% of the Arias intensity as the lower and upper bounds (Trifunac and Brady, 1975), Ds for this waveform is ~1 sec (Figure 12a).

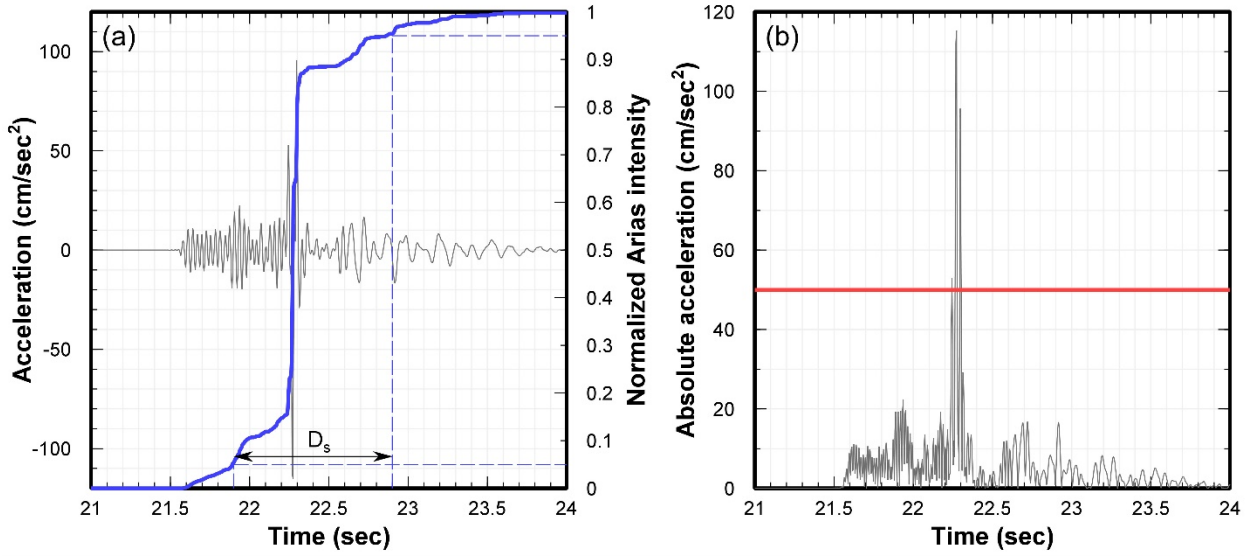

Figure 12. A representative example of recorded accelerogram and its strong shaking duration. (a) Thin black line shows the east–west component of the strong motion waveform from an M 3.0 event with peak ground acceleration of ~115 cm/sec^2 recorded at ~2.6 km from the source at one of the Arc seismograph stations. Solid thick line is the normalized Arias intensity with horizontal dashed lines marking the 5% and 95% of intensity. Ds is the significant duration, as bounded by the vertical dashed lines. (b) Absolute values of acceleration with the solid horizontal line marking the 50 cm/sec^2 threshold in the calculation of bracketed duration. From Babaie Mahani and Kao (2018).

In Figure 12b, the absolute values of acceleration are shown. For ground motion amplitudes above the 50 cm/sec^2 threshold, Db is only a fraction of a second (Figure 12b). Although both the bracketed and significant durations can be used in describing the damage potential of strong ground motion, their interpretations are different. For two accelerograms with identical PGA, the one with longer duration is more damaging. On the other hand, for two accelerograms with identical energy (maximum Arias intensity), the one with shorter duration is likely to cause more damage. In Figures 13 and 14, Ds and Db (at 1 cm/sec^2 threshold) are plotted against distance, magnitude, PGA, and V_{S30} for the two areas of Graham and Septimus. There is a clear

relationship between Ds and hypocentral distance and PGA, that is, Ds systematically increases with distance but decreases with PGA (Figure 13a,c). On the other hand, no significant trend can be observed with respect to the magnitude and Vs_{30} ranges (Figure 13b,d). Db appears to increase with magnitude (Figure 14b) and shows a strong correlation with PGA as well (increases with PGA; Figure 14c), but there are no trends for either distance or Vs_{30} (Figure 14a,d).

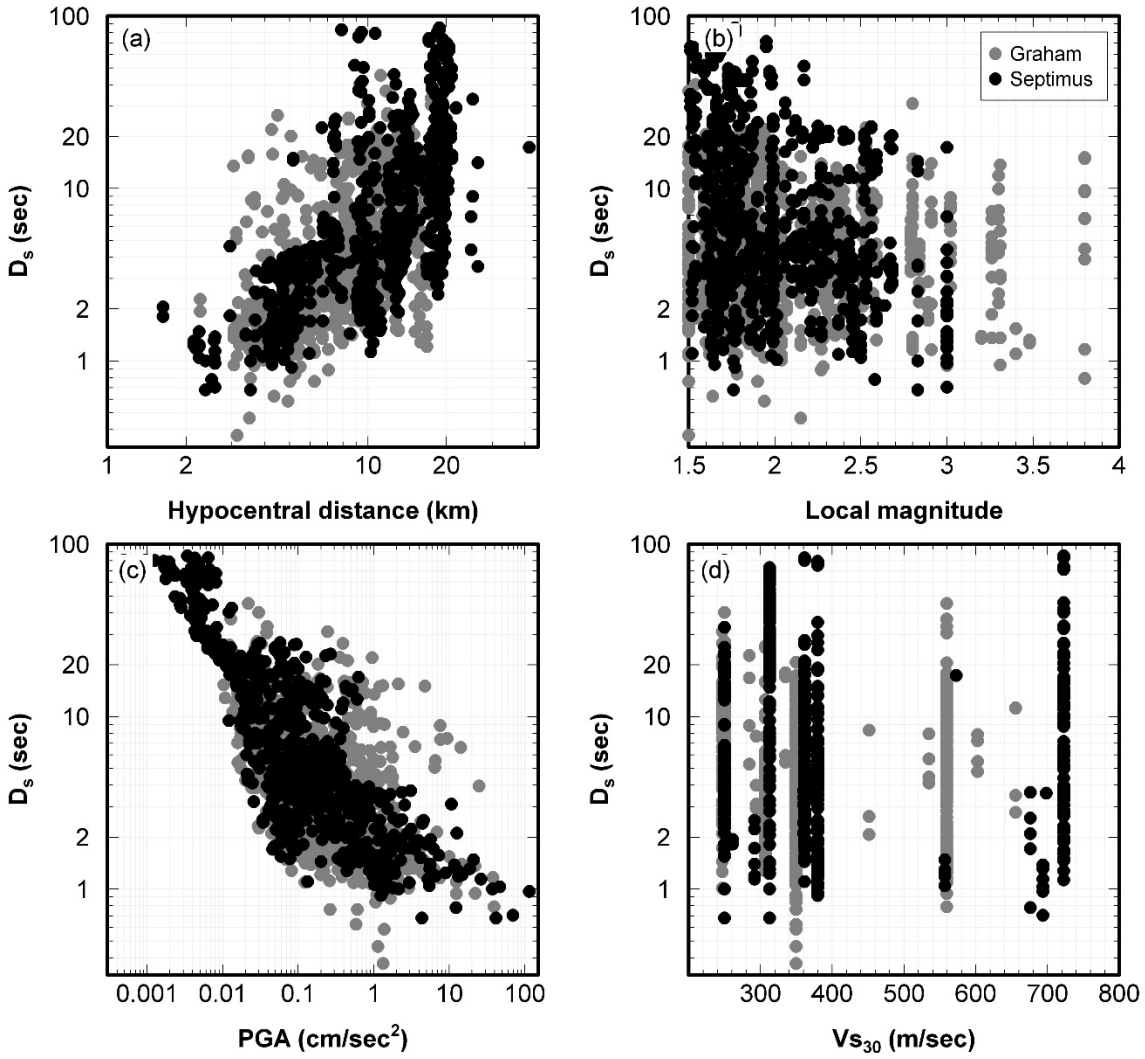

Figure 13. Relationship between significant duration (Ds) and different parameters in the two areas of Graham and Septimus. (a) hypocentral distance; (b) local magnitude; (c) peak ground acceleration (PGA); (d) time-averaged shear-wave velocity in the top 30 m (Vs_{30}). From Babaie Mahani and Kao (2018).

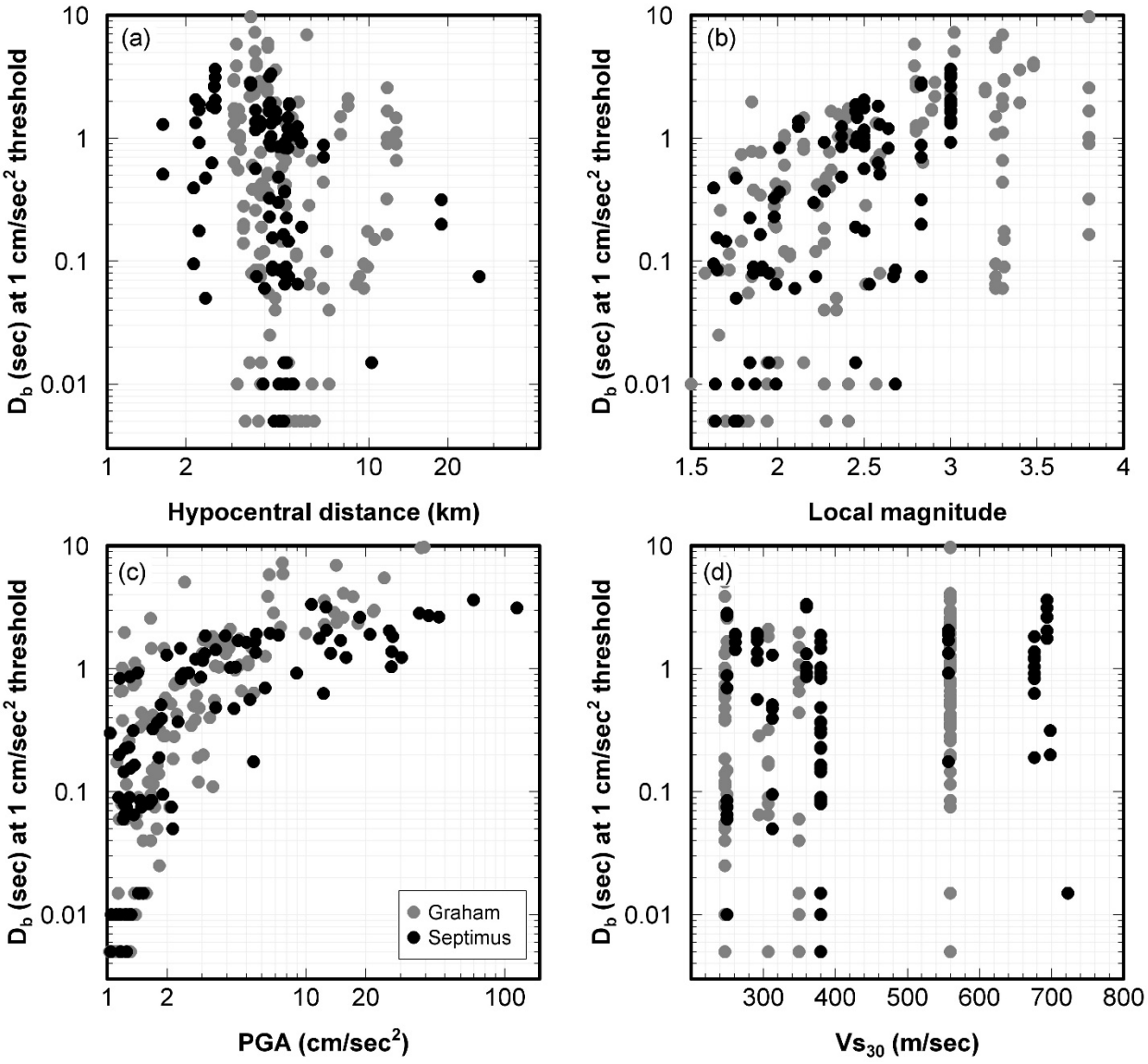

Figure 14. Relationship between bracketed duration (Db) at 1 cm/sec^2 threshold and different parameters in the two areas of Graham and Septimus. (a) hypocentral distance; (b) local magnitude; (c) peak ground acceleration (PGA); (d) time-averaged shear-wave velocity in the top 30 m (Vs_{30}). From Babaie Mahani and Kao (2018).

Seismicity in 2016-2017

Figure 15 shows the events occurred in NE BC between January 2016 and October 2017. Total of 355 events were reported in the NRCan earthquake catalogue with magnitude 0.5-3.9 during this period.

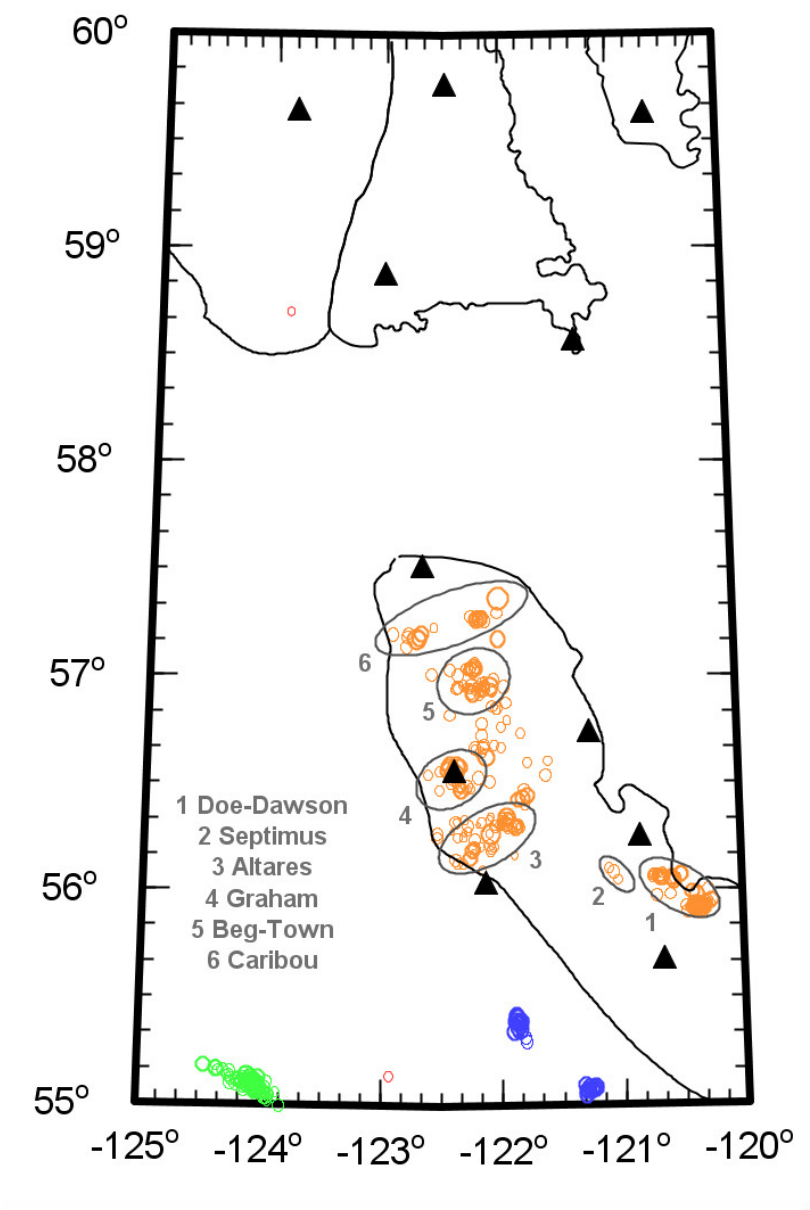

Figure 15. Events reported in the Natural Resources Canada earthquake catalogue in northeast British Columbia between January 2016 and October 2017.

Besides the two events shown with red circle, all earthquakes appear to be clustered across the region. Most of the events occurred in the Montney Play (249 events, orange circle) and clustered in areas as described in the previous report for the BC-OGRIS (Salas, 2016). These clusters are the Doe-Dawson, Septimus, Altares, Graham, Beg-Town, and Caribou (Figure 15). There are also other clusters to the south and southwest of the Montney Play; 40 events occurred

in clusters to the south of the Montney Play (blue circle) and 64 events occurred in a cluster to the southwest of the Montney Play (green circle). The source of earthquakes to the south and southwest of the Montney Play can be either related to quarry blasts or natural.

Figure 16 shows the magnitude distribution of the events shown in Figure 15. Events in the Montney Play follow a normal distribution with an average magnitude of ~2.0, while the two other clusters skew towards higher magnitudes although this can be due to the higher magnitude of completeness for areas outside of the well-covered seismographic network in northeast British Columbia (Figure 3).

Fluid Injection and Induced Seismicity

Babaie Mahani et al. (2017a) conducted a detailed analysis of the seismicity in the Beg-Town area during 2015 with focus on the August 17, 2015 Mw 4.6 event and its connection with fluid injection (hydraulic fracturing and long-term injection of gas and waste-water disposal). Using a comprehensive dataset from industry including 676 events from October 3, 2014 to December 31, 2015, they concluded that these events are better correlated with hydraulic fracturing (correlation coefficient of ~0.17 at confidence level close to 99.7%) than other types of injection (Figure 17). The depths of these events range from 0.5 to 2.5 km and are mostly constrained above the target zone where hydraulic fracturing was taking place. The best-fit moment tensor solution for the Mw 4.6 event gives a predominantly reverse faulting mechanism in the northwest-southeast direction (Figure 18).

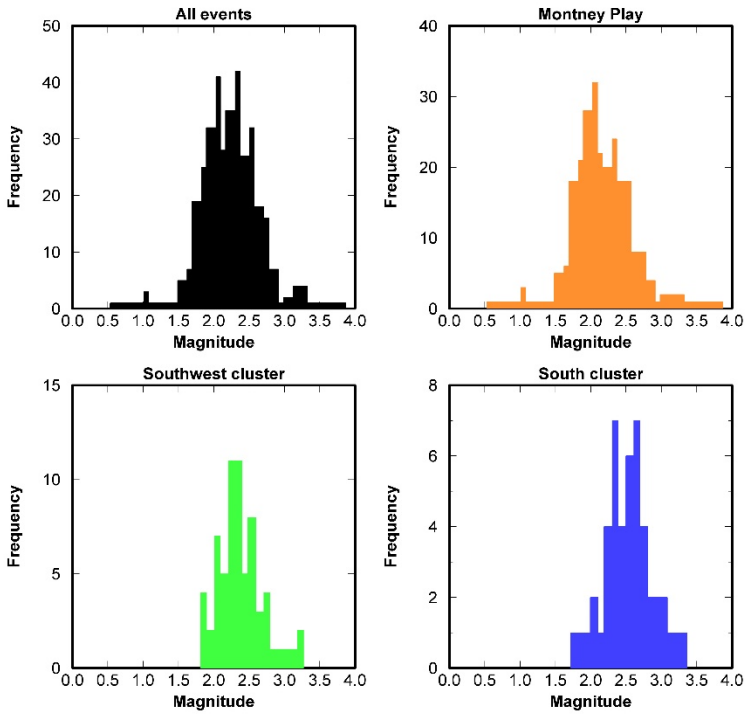

Figure 16. Histogram of the magnitude distribution of the clusters shown in Figure 15. Black shows all the events in northeast British Columbia between January 2016 and October 2017 while orange, green, and blue represent the events in the Montney Play, the cluster to the southwest, and the cluster to the south of the Montney Play, respectively.

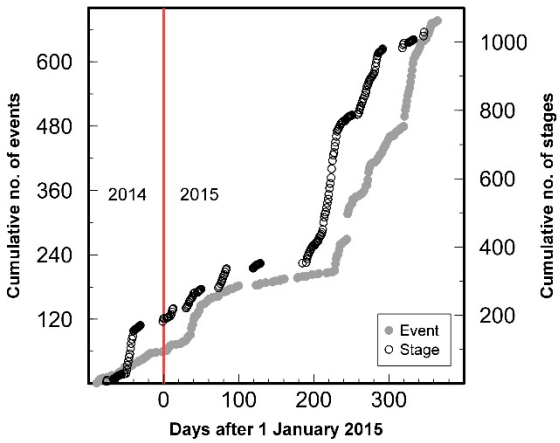

Figure 17. Cumulative numbers of seismic events and hydraulic fracturing stages in the Beg-Town area from October 2014 to the end of 2015. Sharp increase in seismicity correlates remarkably well with the increase in hydraulic fracturing operations. From Babaie Mahani et al. (2017a).

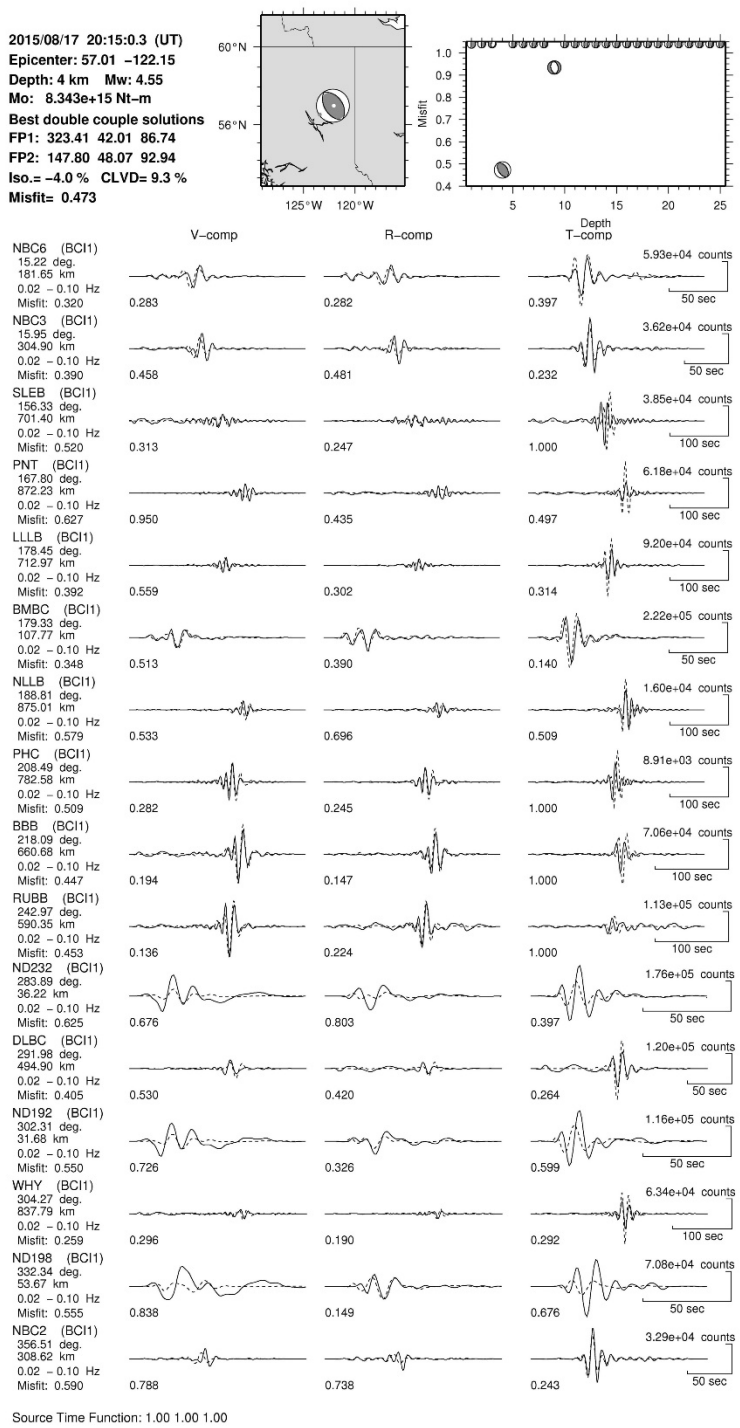

Figure 18. Moment tensor inversion for the Mw 4.6 event on 17 August 2015. A summary of source parameters, map of the epicenter, and the misfit versus depth are shown at the top. Epicenter location is from the Natural Resources Canada catalogue. Focal mechanism is plotted in lower-hemisphere projection with darkened quadrants showing compressional (up) first motions. In the lower panel, synthetic and observed seismograms at each station component used in this inversion are plotted as dashed and solid lines, respectively. V, R, and T, correspond to the vertical, radial, and transverse components, respectively. From Babaie Mahani et al. (2017a).

Communication and Extension Plan

The members of the BC Seismic Research Consortium have presented the following papers or presentations throughout 2016 and 2017.

Presentations

Ali Mahani (Project Seismologist)

Monitoring of Induced Seismicity in northeast BC (2012-2017), Canadian Society for Unconventional Resources Induced Seismicity Workshop, December 5, 2017, Calgary

Ground Motion from Small Induced Earthquakes Recorded at Short Hypocentral Distance in northeast BC, Geoscience BC: Update on Induced Seismicity & Natural Gas Liquids Research, CSUR, Calgary, Alberta, September 19, 2017

Ground Motion Amplitudes in Alberta and northeastern British Columbia, Alberta Energy Regulator Workshop on Induced Seismicity, Calgary, February 16, 2017.

Fluid Injection and Seismic Activity in the northern Montney Play, British Columbia, with Special Reference to the August 17, 2015 Mw 4.6 Induced Earthquake, Microseismic User Group, Calgary, January 30, 2017.

Induced Seismicity in NE BC: An Update, Canadian Induced Seismicity Collaboration Workshop, TransAlta office, Calgary, October 27, 2016.

Performance Evaluation of the Regional Seismograph Network in northeast British Columbia, Canada, for Monitoring of Induced Seismicity, Ali Mahani, Honn Kao, Dan Walker, Jeff Johnson,

and Carlos Salas, Seismological Society of America annual meeting, Reno, Nevada, April 20-22, 2016.

The August 17, 2015 Mw 4.6 Hydraulic Fracturing-Induced Earthquake in Northern Montney Play, British Columbia, Canada, Ali Mahani, Ryan Schultz, Honn Kao, Dan Walker, Jeff Johnson, and Carlos Salas, Seismological Society of America annual meeting, Reno, Nevada, April 20-22, 2016.

Honn Kao

Kao, H., A.B. Mahani, R. Schultz (2016). The Largest Hydraulic Fracturing – Induced Earthquake in Canada: Source Characteristics and Seismic Hazard Implications of the August 17, 2015, Mw 4.6 Earthquake in Northeast British Columbia, Abstract S54B-06, American Geophysical Union annual meeting, December 12-16, 2016, San Francisco, CA.

Wang, B., R.M. Harrington, Y. Liu, and H. Kao (2016). Static stress drop of the largest recorded M 4.6 hydraulic fracturing induced earthquake and its aftershock pattern in the northern Montney Play, British Columbia, Canada, Abstract S43C-2880, American Geophysical Union annual meeting, December 12-16, 2016, San Francisco, CA.

Kao H. (2016). Defining the normal to single out the odd: Baseline studies of regional seismicity for major shale gas basins in Canada, TransAlta Workshop (27 October, Calgary, Alberta).

Kao, H., M. Lamontagne, D. Lavoie, and J.F. Cassidy (2016). Research on oil and gas-related seismicity at Natural Resources Canada, Abstract ESC2016-713, 35th General Assembly of the European Seismological Commission (Sep 4 – 11, Trieste, Italy).

Kao, H. (2016). Natural Resource Canada's Induced Seismicity Research Project, Environmental Geoscience Program Meeting (May 10 and 11, Quebec City).

Kao, H. (2016). Induced Seismicity Associated with Shale Gas Development, webinar presented to all NRCan offices, Environmental Geoscience Program Meeting (May 10 and 11, Quebec City).

Kao, H., A.B. Mahani, D. Walker, G.M. Atkinson, and D.E. Eaton (2016). The first step toward an effective traffic light protocol for induced seismicity: A data-sharing framework for earthquake monitoring in northeast British Columbia, Canada, Seismological Society of America annual meeting, Reno, Nevada, April 20-22, 2016.

Lamontagne, M., D. Lavoie, and H. Kao (2016). Monitoring background level of seismicity in regions with shale oil and gas potential in eastern Canada, Seismological Society of America annual meeting, Reno, Nevada, April 20-22, 2016.

Carlos Salas (Geoscience BC)

CSUR Induced Seismicity Conference, December 9, 2016, Calgary, Alberta.

Induced Seismicity webpage – energy sector feedback, February 25, 2016, Calgary, Alberta.

Induced Seismicity in Northeast BC Forum (OGC-NRCan), January 29, 2016, Sidney, BC.

Stuart Venables (BC Oil and Gas Commission)

Induced Seismicity in BC – Regulatory Response and Case Studies, Michelle Gaucher and Stuart Venables, SPE/SEG Workshop: Injection Induced Seismicity – Engineering Integration, Evaluation and Mitigation, March 28-30, 2016, Fort Worth, Texas.

Induced Seismicity in BC: Regulatory Update, Microseismic User Group Luncheon talk, October 28, 2016.

Understanding Induced Seismicity in Canada: Observations, Research, and Management in British Columbia, Roundtable on Unconventional Hydrocarbon Development, National Academy of Sciences, December 1-2, 2016, Washington, DC.

Jeff Johnson (BC Oil and Gas Commission)

BC Update: Induced Seismicity, Alberta Energy Regulator Workshop on Induced Seismicity, Calgary, February 16, 2017.

Technical Papers

Babaie Mahani, A. and H. Kao (2018). Attenuation of Ground-Motion Amplitudes from Small-Magnitude Earthquakes in the Montney Play, Northeastern British Columbia; in Geoscience BC Summary of Activities 2017, Energy, Geoscience BC, Report 2018-4, p. 15-22.

Babaie Mahani, A. and H. Kao (2018). Ground Motion from M 1.5 to 3.8 Induced Earthquakes at Hypocentral Distance < 45 km in the Montney Play of Northeast British Columbia, Canada, Seismological Research Letters, Vol. 89, No. 1, p. 22-34.

R. Visser, B. Smith, H. Kao, A. Babaie Mahani, J. Hutchinson, and J. McKay (2017). A Comprehensive Earthquake Catalogue for northeastern British Columbia and western Alberta, 2014-2016, Geological Survey of Canada Open File 8335, 28 pages.

H. Kao, A. Babaie Mahani, J. Johnson, and S. Venables (2017). Magnitude Calculations for Induced Seismicity in the NE BC Oil and Gas Operating Area, 7 pages.

Babaie Mahani, A., R. Schultz, H. Kao, D. Walker, J. Johnson, and C. Salas (2017). Fluid Injection and Seismic Activity in the Northern Montney Play, British Columbia, Canada, with Special Reference to the 17 August 2015 Mw 4.6 Induced Earthquake, Bulletin of Seismological society of America, April 2017, V. 107, No. 2, p. 542-552.

Rashedi, H., and A. B. Mahani (2017). Data Analysis of Induced Seismicity in Western Canada, CSEG Recorder, January, page 26-28.

Babaie Mahani, A., H. Kao, J. Johnson, and C. Salas (2017). Ground Motion from the August 17, 2015, Moment Magnitude 4.6 Earthquake Induced by Hydraulic Fracturing in Northeastern British Columbia; in Geoscience BC Summary of Activities 2016, Geoscience BC, Report 2017-1, p. 9–14.

Babaie Mahani, A., H. Kao, D. Walker, J. Johnson, and C. Salas (2016). Performance Evaluation of the Regional Seismograph Network in Northeast British Columbia, Canada, for Monitoring of Induced Seismicity, Seismological Research Letters, May/June 2016, V. 87, p. 648-660.

Babaie Mahani, A., Kao, H., Walker, D., Johnson, J. and Salas, C. (2016): Regional Monitoring of Induced Seismicity in Northeastern British Columbia; in Geoscience BC Summary of Activities 2015, Geoscience BC, Report 2016-1, p. 79-88.

H. Kao, D. W. Eaton, G. M. Atkinson, S. Maxwell, and A. Babaie Mahani (2016). Technical Meeting on the Traffic Light Protocols (TLP) for Induced Seismicity: Summary and Recommendations, Geological Survey of Canada Open File 8075.

Current Research

The following projects are currently being performed by the members of the BC Seismic Research Consortium.

Reconstruction of clipped waveforms

An advantage of the data provided by the seismographic stations operated by energy companies is the availability of ground motion amplitudes at close distances to the operation and source of the earthquakes. However, the close distance of these stations can cause some sensors to clip at large ground motion amplitudes. This is the main reason for the requirement of BC Oil and Gas Commission for accelerometer deployment close to the well pads since accelerometers are designed to have higher clip level than the broadband seismometers. Figure 19 shows an example of clipping on the Progress Energy seismographic stations from large ground motion of the Mw 4.6 event on August 17, 2015 in the northern Montney Play (Babaie Mahani et al., 2017b).

Sensors located as far as 40 km were clipped (Figure 19, left column). For the smaller event on September 2, 2017 with Mw 3.2 only the station located at distance ~7.5 was clipped (Figure 19, middle column), while none of the sensors that recorded the Mw 3.0 on August 17, 2015 (3 hour after the main shock) were clipped (Figure 19, right column). Using the unclipped ground motion from the M_w 3.0 aftershock, Babaie Mahani et al. (2017b) estimated that PGA from the M_w 4.6 event could have been as high as ~173 cm/sec^2 (~17% g) at an epicentral distance of ~5 km (Figure 20).

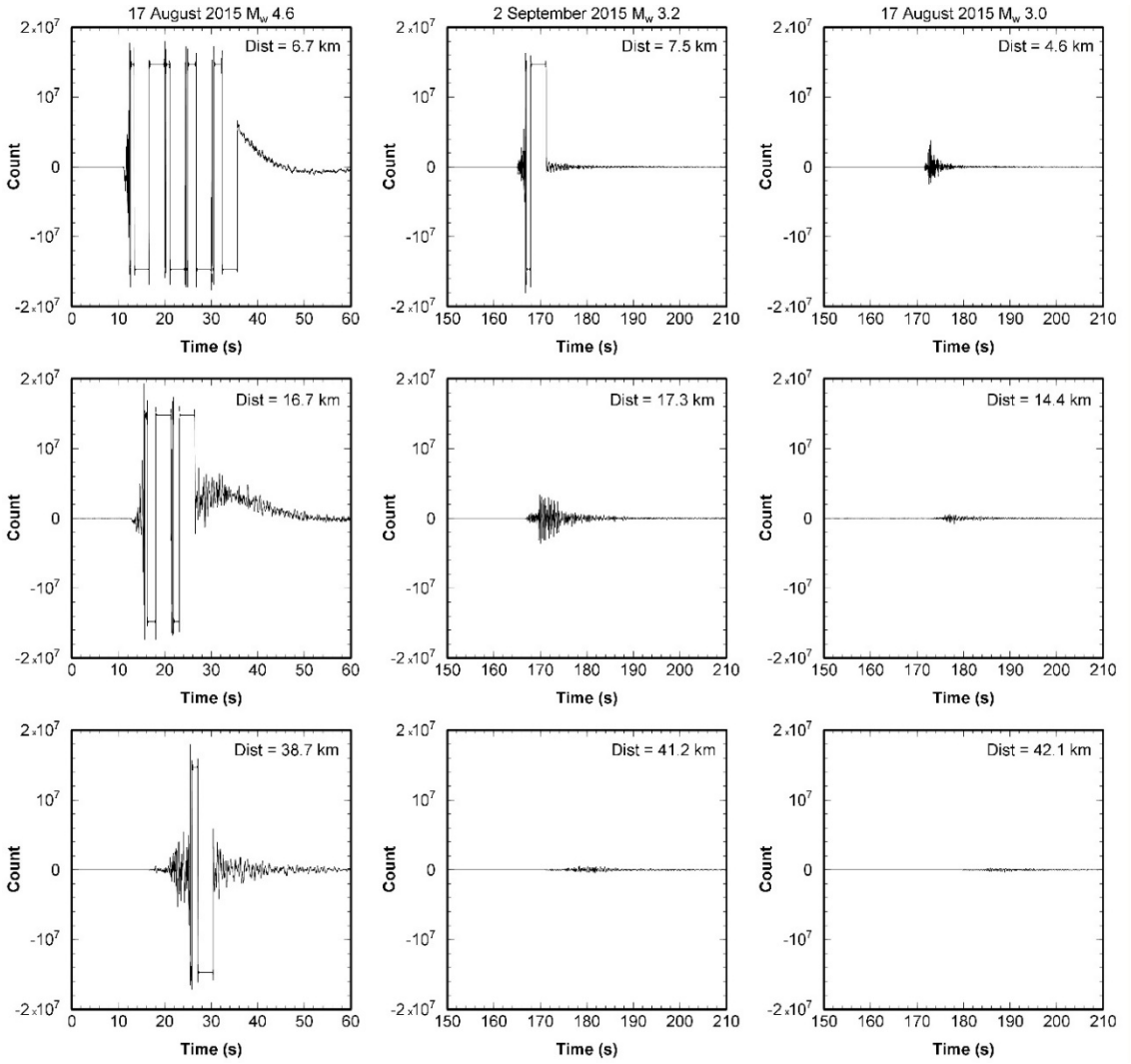

Figure 19. Sample raw seismograms (E-W component) from three largest induced earthquakes in the northern Montney Play of British Columbia. Seismic waveform data were recorded by the broadband seismographic stations operated by Progress Energy. For the August 17, 2015 M_w 4.6 event, waveform amplitudes were clipped at distances up to ~40 km. In contrast, only one station located near the September 2, 2017 M_w 3.2 epicenter had clipped waveforms. From Babaie Mahani et al. (2017b).

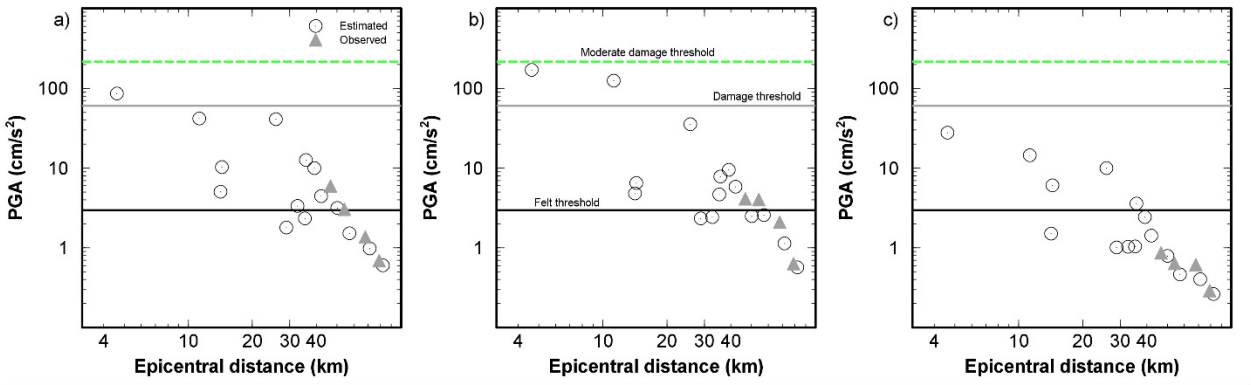

Figure 20. Estimated peak ground acceleration (PGA) for the E-W (a), N-S (b), and vertical (c) components of the August 17, 2015 M_w 4.6 event from the unclipped ground motion data from the smaller M_w 3.0 event. PGA as high as ~173 cm/sec^2 (~17% g) is estimated for places close to the epicenter (~5 km or less). The three thresholds (felt, damage, moderate damage) are taken from Worden et al. (2012). Our estimated PGA values are remarkably consistent with the observed ones from unclipped waveforms at distances >40 km (shown as gray triangles). From Babaie Mahani et al. (2017b).

Although estimated PGA values were obtained for the clipped waveforms from the Mw 4.6 event, other parameters such as PSA at several frequencies and duration of the strong motion from this large induced event can be important in characterizing ground motion amplitudes. For this reason, with collaboration by researchers from Western University (Gail Atkinson and Hadi Ghofrani), more robust methodologies are being conducted to reconstruct the clipped time series of the Mw 4.6 event. The established methodology can also serve as a template for other cases of clipped motions from large events for which the data can be unusable otherwise.

Conclusions

Since 2013, total of 23 broadband seismographic stations have been installed across NEBC and environs to better monitor the induced events and their relation with oil and gas activities. This significant improvement in the monitoring capability of the regional network has resulted in the

accurate detection of small magnitude earthquakes across the region; a task which was not possible before then. The magnitude of completeness is ~2 which have been improved by 1 unit of magnitude since 2013. The minimum detectable magnitude by the current network can be as low as ~0.4 providing detailed information on the geological structures responsible for the generation of induced earthquakes. As the result of the improved network location resolution has also been enhanced to the point that small magnitude induced earthquakes can be correlated with injection operations more accurately. Besides the improvement in the routine detection of earthquakes across NE BC, the enhanced network provides data for scientific studies such as analysis of ground motion amplitudes at close distances to the injection operations and infrastructure.

Acknowledgement

We thank Ryan Schultz from Alberta Energy Regulator and Hadi Ghofrani from Western University for their help in the analysis of epicentral uncertainty.

References

Arias, A. (1970). A Measure of Earthquake Intensity, in seismic Design for Nuclear Power Plants, ed. Hansen, R. (MIT press, Cambridge, Massachusetts), pp. 438-483.

Babaie Mahani, A. and H. Kao (2018). Ground Motion from M 1.5 to 3.8 Induced Earthquakes at Hypocentral Distance < 45 km in the Montney Play of Northeast British Columbia, Canada, Seismological Research Letters, Vol. 89, No. 1, p. 22-34.

Babaie Mahani, A., R. Schultz, H. Kao, D. Walker, J. Johnson, and C. Salas (2017a). Fluid Injection and Seismic Activity in the Northern Montney Play, British Columbia, Canada, with

Special Reference to the 17 August 2015 Mw 4.6 Induced Earthquake, Bulletin of Seismological society of America, April 2017, V. 107, No. 2, p. 542-552.

Babaie Mahani, A., H. Kao, J. Johnson, and C. Salas (2017b). Ground Motion from the August 17, 2015, Moment Magnitude 4.6 Earthquake Induced by Hydraulic Fracturing in Northeastern British Columbia; in Geoscience BC Summary of Activities 2016, Geoscience BC, Report 2017-1, p. 9–14.

Babaie Mahani, A., H. Kao, D. Walker, J. Johnson, and C, Salas (2016). Performance Evaluation of the Regional Seismograph Network in Northeast British Columbia, Canada, for Monitoring of Induced Seismicity, Seismological Research Letters, V. 87, 648-660.

Bommer, J. J., and A. Martinez-Pereira (1999). The Effective Duration of Earthquake Strong Motion, Journal of Earthquake Engineering, V. 3, No. 2, 127-172.

Nakamura, Y. (1989). A method for dynamic characteristics estimation of subsurface using microtremor on the ground surface, Q. Rep. Railway Tech. Res. Inst. V. 30, no. 1, 25-33.

Salas, C. (2016). BC-OGRIS 2015-2016 Final Report for Year 4 of the Induced Seismicity Monitoring Project (ISMP), 38 pages.

Salas, C. J., and D. Walker (2014). Update on Regional Seismograph Network in Northeastern British Columbia (NTS 094C, G, I, O, P); in Geoscience BC Summary of Activities 2013, Geoscience BC, Report 2014-1, p. 123-126.

Salas, C. J., D. Walker, and H. Kao (2013). Creating a Regional Seismograph Network in Northeast British Columbia to Study the Effect of Induced Seismicity from Unconventional Gas

Completions (NTS 094C, G, I, O, P); in Geoscience BC Summary of Activities 2012, Geoscience BC, Report 2013-1, p. 131-134.

Schultz, R., V. Stern, Y. J. Gu, and D. Eaton (2015). Detection threshold and location resolution of the Alberta Geological Survey Earthquake Catalogue, Seismol. Res. Lett. V. 86, 385-397.

Trifunac, M. D., and A. G. Brady (1975). A study on the duration of strong earthquake ground motion, Bull. Seismol. Soc. Am. V. 65, 581–626.

Worden, C. B., M. C. Gerstenberger, D. A. Rhoades, and D. J. Wald (2012). Probabilistic Relationships between Ground-Motion Parameters and Modified Mercalli Intensity in California, Bulletin of Seismological Society of America, V. 102, 204-221.

Appendix A: Earthquakes between January 2016 and October 2017

Date	Time (UTC)	Latitude	Longitude	Depth	Depth type	Mag	Mag type
2017/09/28	18:18:16	55.390	-121.891	0.0	Fixed	2.5	ML
2017/09/28	17:51:11	55.071	-121.318	0.0	Fixed	2.6	ML
2017/09/24	17:44:46	55.063	-123.970	10.0	Fixed	2.5	ML
2017/09/24	01:48:01	55.363	-121.888	10.0	Fixed	2.4	ML
2017/09/10	18:18:03	55.351	-121.902	0.0	Fixed	2.8	ML
2017/09/06	22:08:52	55.420	-121.876	1.0	Fixed	2.7	ML
2017/09/04	17:41:52	55.055	-121.314	0.0	Fixed	2.7	ML
2017/09/01	02:35:00	55.901	-120.455	1.0	Fixed	2.3	ML
2017/08/30	23:03:28	55.908	-120.350	1.0	Fixed	2.7	ML
2017/08/27	23:11:36	55.984	-120.707	11.4	Calculated	2.3	ML
2017/08/27	22:17:17	55.427	-121.885	0.0	Fixed	2.3	ML
2017/08/24	22:13:14	55.398	-121.874	0.0	Fixed	2.2	ML
2017/08/17	02:05:44	55.093	-121.242	12.9	Calculated	2.5	ML
2017/08/09	03:47:25	56.001	-120.280	1.0	Fixed	2.2	ML
2017/08/07	23:18:12	55.392	-121.858	1.0	Fixed	2.0	ML
2017/08/07	22:31:28	55.073	-121.301	0.0	Fixed	2.3	ML
2017/08/05	22:18:31	55.380	-121.851	0.0	Fixed	2.2	ML
2017/08/05	18:50:10	56.107	-121.108	1.0	Fixed	2.0	ML
2017/08/02	21:52:24	55.059	-123.862	13.0	Calculated	2.0	ML
2017/08/01	02:05:24	55.081	-121.242	0.0	Calculated	2.5	ML

2017/07/26	21:42:04	55.112	-124.117	0.0	Calculated	2.1	ML
2017/07/11	13:14:59	55.986	-120.598	10.0	Fixed	2.1	ML
2017/07/07	22:20:50	55.350	-121.859	5.0	Fixed	1.7	ML
2017/06/21	12:03:51	55.934	-120.257	1.0	Fixed	1.6	ML
2017/06/19	03:28:21	56.612	-121.609	10.0	Fixed	1.8	ML
2017/06/19	01:35:49	55.372	-121.842	10.0	Fixed	1.9	ML
2017/06/10	22:04:44	55.981	-120.383	0.0	Calculated	2.6	ML
2017/06/10	13:37:00	55.994	-120.418	1.7	Calculated	2.5	ML
2017/06/08	21:28:27	55.108	-124.009	7.4	Calculated	2.2	ML
2017/06/08	20:22:18	56.559	-122.399	1.0	Fixed	3.3	ML
2017/06/05	22:11:55	55.047	-121.326	0.0	Fixed	2.3	ML
2017/06/01	18:10:07	55.404	-121.849	0.0	Fixed	2.0	ML
2017/05/27	01:54:18	55.072	-121.270	8.4	Calculated	2.5	ML
2017/05/18	02:06:11	55.081	-121.311	0.0	Fixed	2.4	ML
2017/05/15	19:44:08	55.144	-122.936	1.0	Fixed	1.9	ML
2017/05/14	21:36:20	55.132	-124.010	0.0	Fixed	2.7	ML
2017/04/28	02:13:39	55.067	-121.321	1.0	Fixed	2.2	ML
2017/04/27	18:10:01	55.372	-121.851	5.0	Fixed	2.3	ML
2017/04/25	22:01:30	55.082	-124.071	0.0	Fixed	2.0	ML
2017/04/21	07:47:09	56.571	-122.442	5.0	Fixed	3.0	ML
2017/04/20	22:38:56	55.121	-124.075	0.0	Fixed	2.3	ML
2017/04/19	19:07:57	56.588	-122.436	1.0	Fixed	3.2	ML
2017/04/18	18:24:56	55.082	-121.297	0.0	Fixed	2.1	ML
2017/04/18	18:22:25	55.403	-121.855	1.0	Fixed	2.2	ML
2017/04/17	22:34:26	55.071	-123.958	0.0	Fixed	2.0	ML

2017/04/11	16:36:14	55.931	-120.469	1.0	Fixed	2.1	ML
2017/04/11	05:48:11	56.656	-122.173	8.6	Calculated	2.1	ML
2017/04/11	01:53:27	55.075	-121.272	4.4	Calculated	2.6	ML
2017/04/10	22:59:26	55.117	-124.043	0.0	Fixed	2.6	ML
2017/04/10	20:17:33	55.919	-120.376	5.6	Calculated	2.5	ML
2017/04/10	19:09:25	55.903	-120.396	1.0	Fixed	2.2	ML
2017/04/10	14:47:42	55.419	-121.891	1.0	Fixed	2.6	ML
2017/04/10	02:10:25	55.917	-120.385	3.0	Calculated	2.5	ML
2017/04/09	21:08:48	56.093	-121.067	9.5	Calculated	2.4	ML
2017/04/09	04:02:25	55.941	-120.391	3.0	Calculated	2.7	ML
2017/04/09	03:05:09	55.920	-120.413	0.0	Calculated	2.5	ML
2017/04/09	00:39:49	55.917	-120.372	8.0	Calculated	2.5	ML
2017/04/08	13:16:13	55.932	-120.408	6.8	Calculated	2.4	ML
2017/04/08	01:03:01	55.918	-120.395	5.4	Calculated	2.5	ML
2017/04/06	21:42:03	55.935	-120.385	5.0	Fixed	2.1	ML
2017/04/05	23:19:01	55.932	-120.369	2.0	Calculated	2.4	ML
2017/04/05	23:10:22	55.358	-121.859	2.2	Calculated	3.1	ML
2017/04/05	20:24:04	55.922	-120.388	3.3	Calculated	2.5	ML
2017/04/05	20:14:46	55.928	-120.386	3.5	Calculated	2.5	ML
2017/04/05	18:44:20	55.915	-120.378	7.0	Calculated	2.5	ML
2017/04/05	18:03:45	55.918	-120.409	1.0	Fixed	2.5	ML
2017/04/05	17:59:30	55.920	-120.368	1.0	Fixed	2.4	ML
2017/04/05	14:40:25	55.920	-120.376	1.0	Fixed	2.7	ML
2017/04/05	09:38:59	55.930	-120.380	3.0	Calculated	2.8	ML
2017/04/04	21:42:50	55.094	-124.006	0.0	Fixed	2.7	ML

2017/03/27	21:50:17	55.050	-123.925	0.0	Fixed	2.4	ML
2017/03/27	01:50:43	55.080	-121.285	1.0	Fixed	2.3	ML
2017/03/26	18:23:50	55.403	-121.853	5.0	Fixed	2.5	ML
2017/03/26	10:48:52	56.299	-121.884	6.1	Calculated	2.6	ML
2017/03/20	21:37:45	55.088	-124.027	0.0	Fixed	2.3	ML
2017/03/20	02:23:13	55.320	-121.809	7.7	Calculated	2.3	ML
2017/03/17	01:33:00	55.954	-120.257	7.0	Calculated	2.5	ML
2017/03/16	20:28:00	56.828	-122.433	7.4	Calculated	2.1	ML
2017/03/16	19:58:22	55.914	-120.327	5.0	Fixed	2.5	ML
2017/03/15	16:07:08	57.148	-122.805	1.0	Fixed	2.4	Mw
2017/03/14	21:58:06	55.113	-124.140	0.0	Fixed	2.5	ML
2017/03/10	22:14:06	55.386	-121.871	0.0	Fixed	2.6	ML
2017/03/10	01:21:34	55.096	-124.010	7.0	Calculated	2.4	ML
2017/03/07	01:29:12	55.368	-121.856	1.0	Fixed	2.3	ML
2017/03/04	22:36:16	55.054	-123.948	0.0	Fixed	2.2	ML
2017/03/02	22:11:16	55.090	-121.262	5.0	Fixed	2.5	ML
2017/02/27	22:16:12	56.673	-122.223	5.0	Fixed	2.4	ML
2017/02/25	00:45:03	56.669	-122.226	7.5	Calculated	1.7	ML
2017/02/20	22:11:45	55.102	-121.324	1.0	Fixed	2.7	ML
2017/02/16	13:05:01	56.679	-122.160	5.8	Calculated	2.3	ML
2017/02/15	19:16:49	55.188	-124.459	0.0	Fixed	2.5	ML
2017/02/08	00:45:11	55.356	-121.841	5.0	Fixed	2.4	ML
2017/02/06	20:51:09	56.075	-120.510	7.2	Calculated	2.6	ML
2017/02/03	23:15:10	56.864	-122.034	5.0	Fixed	2.3	ML
2017/02/03	15:26:54	57.198	-122.797	7.9	Calculated	2.3	ML

2017/02/02	23:38:48	55.110	-124.068	0.0	Fixed	2.8	ML
2017/02/01	23:24:40	55.398	-121.897	1.0	Fixed	2.6	ML
2017/01/30	21:01:30	56.075	-120.509	5.0	Fixed	2.4	ML
2017/01/24	21:54:44	55.085	-121.303	0.0	Fixed	2.6	ML
2017/01/17	21:21:51	55.123	-124.072	0.0	Fixed	3.2	ML
2017/01/17	19:00:32	57.213	-122.678	5.0	Fixed	2.7	ML
2017/01/16	14:26:04	56.066	-120.656	6.1	Calculated	2.7	ML
2017/01/15	22:40:14	55.107	-124.234	0.0	Fixed	2.4	ML
2017/01/15	22:17:20	55.398	-121.870	1.6	Calculated	2.7	ML
2017/01/15	10:07:50	56.315	-121.862	5.0	Fixed	2.0	ML
2017/01/14	10:50:26	56.063	-120.679	6.7	Calculated	2.5	ML
2017/01/12	23:09:44	56.056	-120.667	1.1	Calculated	2.1	ML
2017/01/12	18:48:53	56.062	-120.694	5.0	Fixed	2.1	ML
2017/01/12	07:22:22	56.068	-120.672	4.3	Calculated	1.7	ML
2017/01/12	07:18:54	56.083	-120.661	8.2	Calculated	2.0	ML
2017/01/11	19:15:42	55.126	-124.126	0.0	Fixed	1.9	ML
2017/01/09	22:56:45	55.299	-121.802	10.0	Fixed	2.4	ML
2017/01/05	22:49:10	55.183	-124.356	0.0	Fixed	2.0	ML
2017/01/02	23:28:57	55.096	-124.067	0.0	Fixed	2.3	ML
2016/12/30	00:06:24	56.591	-122.379	1.0	Fixed	3.2	ML
2016/12/23	22:28:59	55.424	-121.890	5.0	Fixed	2.6	ML
2016/12/17	22:45:28	55.173	-124.350	0.0	Fixed	2.7	ML
2016/12/12	23:18:53	55.086	-124.016	0.0	Fixed	2.3	ML
2016/12/06	06:52:43	56.438	-121.820	4.4	Calculated	2.6	ML
2016/12/03	05:13:55	56.268	-122.089	14.1	Calculated	3.4	ML

2016/11/30	06:07:10	56.630	-122.132	8.1	Calculated	2.9	ML
2016/11/19	22:45:48	55.394	-121.854	5.0	Fixed	2.8	ML
2016/11/17	02:55:20	57.191	-122.699	8.6	Calculated	2.7	ML
2016/11/16	00:20:19	55.099	-124.042	0.0	Fixed	2.6	ML
2016/11/12	16:22:30	57.204	-122.924	11.2	Calculated	2.4	ML
2016/11/10	06:24:54	56.311	-122.051	10.0	Fixed	2.3	ML
2016/11/10	05:58:34	56.353	-121.954	5.4	Calculated	3.1	ML
2016/11/03	09:05:44	57.185	-122.028	7.7	Calculated	2.8	ML
2016/11/02	23:38:34	55.098	-124.038	0.0	Fixed	2.3	ML
2016/10/26	04:04:30	56.058	-120.581	6.2	Calculated	2.6	ML
2016/10/25	22:25:41	56.060	-120.557	8.2	Calculated	2.3	ML
2016/10/25	20:49:52	56.061	-120.585	5.6	Calculated	2.5	ML
2016/10/23	14:09:50	56.049	-120.585	8.9	Calculated	2.4	ML
2016/10/21	15:58:21	56.044	-120.562	3.2	Calculated	2.6	ML
2016/10/19	14:26:31	57.210	-122.786	1.0	Fixed	2.1	ML
2016/10/18	01:14:16	56.744	-121.834	8.2	Calculated	2.0	ML
2016/10/16	03:27:53	57.184	-122.718	6.2	Calculated	3.5	ML
2016/10/10	09:19:29	56.456	-121.788	5.6	Calculated	2.7	ML
2016/10/05	00:30:43	56.688	-122.147	6.4	Calculated	2.4	ML
2016/10/04	05:35:16	56.944	-122.164	6.6	Calculated	2.3	ML
2016/10/04	04:38:39	56.928	-122.245	12.4	Calculated	2.8	ML
2016/10/04	04:21:04	56.478	-122.336	7.7	Calculated	2.7	ML
2016/09/13	17:42:36	55.154	-124.119	0.0	Fixed	1.8	ML
2016/09/03	17:41:54	55.078	-124.013	0.0	Calculated	2.2	ML
2016/08/09	12:06:59	56.272	-122.540	10.6	Calculated	2.2	ML

2016/08/08	01:49:44	56.330	-122.391	8.8	Calculated	2.3	ML
2016/08/06	17:43:20	55.091	-124.126	0.0	Fixed	2.4	ML
2016/08/05	02:36:28	56.306	-122.279	9.2	Calculated	2.2	ML
2016/08/04	21:37:53	56.329	-122.379	7.7	Calculated	1.5	ML
2016/08/04	21:29:15	56.968	-122.320	1.8	Calculated	2.0	ML
2016/08/04	19:27:34	56.077	-120.719	6.4	Calculated	1.7	ML
2016/08/04	19:19:20	56.077	-120.738	4.5	Calculated	1.8	ML
2016/08/04	16:47:57	56.074	-120.739	4.2	Calculated	2.0	ML
2016/08/04	16:20:04	56.070	-120.746	5.3	Calculated	2.0	ML
2016/08/04	13:29:05	56.358	-122.088	3.4	Calculated	1.5	ML
2016/08/04	11:43:59	56.081	-120.699	3.9	Calculated	1.8	ML
2016/08/04	11:16:25	56.084	-120.725	6.2	Calculated	1.8	ML
2016/08/04	08:15:09	56.066	-120.749	3.6	Calculated	1.9	ML
2016/08/01	18:53:25	56.957	-122.269	2.4	Calculated	1.9	ML
2016/07/30	23:30:01	55.117	-124.091	4.6	Calculated	2.4	ML
2016/07/26	02:13:13	56.339	-122.315	8.2	Calculated	1.7	ML
2016/07/25	04:26:43	56.361	-121.993	0.1	Calculated	1.6	ML
2016/07/24	00:39:56	56.853	-122.041	7.2	Calculated	1.7	ML
2016/07/20	21:49:35	55.105	-124.038	0.0	Fixed	3.2	ML
2016/07/19	22:42:05	55.936	-120.304	3.7	Calculated	2.2	ML
2016/07/19	07:41:22	55.928	-120.329	3.7	Calculated	2.0	ML
2016/07/19	07:09:44	55.919	-120.326	10.1	Calculated	2.1	ML
2016/07/19	05:55:02	55.927	-120.328	4.7	Calculated	2.3	ML
2016/07/18	12:37:50	55.927	-120.326	3.6	Calculated	2.4	ML
2016/07/18	06:50:27	55.921	-120.333	6.6	Calculated	2.1	ML

2016/07/17	14:35:51	55.925	-120.341	15.7	Calculated	2.0	ML
2016/07/17	11:43:11	55.929	-120.294	6.0	Calculated	2.2	ML
2016/07/17	10:28:40	55.928	-120.328	7.2	Calculated	2.2	ML
2016/07/15	04:17:28	56.731	-122.167	11.3	Calculated	2.4	ML
2016/07/14	14:41:34	56.872	-122.081	9.5	Calculated	2.1	ML
2016/07/12	21:08:39	57.374	-122.023	6.2	Calculated	3.9	Mw
2016/07/12	18:43:21	56.963	-122.372	9.1	Calculated	2.3	ML
2016/07/12	16:12:00	56.954	-122.379	9.3	Calculated	2.1	ML
2016/07/12	15:50:16	56.952	-122.370	2.5	Calculated	2.0	ML
2016/07/12	09:15:23	55.916	-120.349	6.1	Calculated	1.9	ML
2016/07/12	05:45:49	55.947	-120.330	11.1	Calculated	1.8	ML
2016/07/11	14:39:44	55.954	-120.284	2.1	Calculated	1.9	ML
2016/07/11	13:13:11	55.932	-120.315	11.5	Calculated	1.9	ML
2016/07/11	09:54:42	55.932	-120.302	6.3	Calculated	2.3	ML
2016/07/11	05:12:17	55.933	-120.316	6.7	Calculated	2.0	ML
2016/07/11	01:43:56	55.922	-120.326	5.1	Calculated	1.8	ML
2016/07/11	00:20:16	55.938	-120.296	2.6	Calculated	1.7	ML
2016/07/10	15:56:10	55.926	-120.318	4.2	Calculated	2.0	ML
2016/07/10	11:10:02	55.945	-120.340	2.7	Calculated	2.1	ML
2016/07/08	13:15:18	55.928	-120.315	7.9	Calculated	2.2	ML
2016/07/08	08:13:17	56.508	-122.377	7.8	Calculated	1.8	ML
2016/07/08	08:11:01	55.944	-120.296	7.0	Calculated	2.0	ML
2016/07/08	07:16:33	55.944	-120.310	6.2	Calculated	2.4	ML
2016/07/03	21:48:03	55.081	-124.040	6.7	Calculated	2.6	ML
2016/07/02	03:36:05	58.710	-123.857	1.0	Fixed	1.6	ML

2016/06/19	04:27:39	56.543	-122.424	0.3	Calculated	1.7	ML
2016/06/17	05:07:29	57.017	-122.243	6.1	Calculated	1.5	ML
2016/06/16	06:36:33	56.320	-121.860	4.2	Calculated	2.1	ML
2016/06/14	10:04:59	56.175	-121.893	10.0	Fixed	1.5	ML
2016/06/13	01:26:26	57.015	-122.371	1.0	Fixed	2.4	ML
2016/06/08	17:05:21	56.538	-122.404	1.0	Fixed	1.7	ML
2016/06/08	14:08:17	56.316	-121.988	6.6	Calculated	1.9	ML
2016/06/04	21:39:35	55.057	-124.019	13.5	Calculated	2.0	ML
2016/06/03	14:01:05	56.330	-122.168	6.4	Calculated	1.9	ML
2016/06/01	22:31:16	55.101	-124.195	0.0	Fixed	2.3	ML
2016/06/01	09:04:13	57.044	-122.264	1.0	Fixed	1.9	ML
2016/05/28	00:55:57	55.069	-124.126	16.2	Calculated	2.2	ML
2016/05/20	06:41:29	56.285	-122.287	15.0	Fixed	1.6	ML
2016/05/20	00:10:56	56.259	-122.325	18.6	Calculated	1.7	ML
2016/05/16	04:02:23	56.331	-121.989	6.6	Calculated	1.7	ML
2016/05/16	00:53:52	55.126	-124.162	0.0	Fixed	2.1	ML
2016/05/14	17:57:20	55.092	-124.018	8.0	Calculated	2.5	ML
2016/05/12	10:43:04	56.322	-122.006	9.3	Calculated	1.7	ML
2016/05/10	16:37:56	56.549	-121.623	7.0	Calculated	2.3	ML
2016/05/02	06:21:13	56.583	-122.345	7.2	Calculated	2.6	ML
2016/05/01	20:52:57	55.031	-123.955	14.9	Calculated	2.2	ML
2016/05/01	05:54:05	56.341	-121.950	4.6	Calculated	2.2	ML
2016/04/28	19:43:24	56.576	-122.404	19.1	Calculated	1.8	ML
2016/04/28	19:09:18	56.563	-122.526	10.7	Calculated	2.0	ML
2016/04/28	19:06:55	56.550	-122.618	11.3	Calculated	2.0	ML

2016/04/27	10:18:06	56.350	-121.951	8.0	Calculated	1.9	ML
2016/04/25	18:07:39	55.128	-124.226	0.0	Fixed	2.3	ML
2016/04/25	16:08:45	56.253	-122.374	7.3	Calculated	1.8	ML
2016/04/25	11:05:47	56.929	-122.253	12.9	Calculated	1.9	ML
2016/04/25	06:41:21	56.579	-122.416	0.0	Fixed	1.9	ML
2016/04/21	21:40:14	55.156	-124.243	0.0	Fixed	2.2	ML
2016/04/21	14:43:37	56.990	-122.142	5.0	Fixed	1.7	ML
2016/04/19	21:33:48	55.164	-124.332	1.0	Fixed	2.1	ML
2016/04/12	21:44:57	55.162	-124.299	0.0	Fixed	2.2	ML
2016/04/09	06:21:05	56.968	-122.144	10.5	Calculated	1.9	ML
2016/04/07	21:53:25	55.057	-123.917	0.0	Fixed	1.9	ML
2016/04/06	14:07:03	56.527	-122.403	6.8	Calculated	2.1	ML
2016/04/05	22:17:49	55.122	-124.171	5.0	Fixed	2.5	ML
2016/03/30	13:39:50	56.955	-122.298	13.7	Calculated	1.6	ML
2016/03/29	12:53:51	56.340	-121.999	1.0	Fixed	1.0	ML
2016/03/29	03:39:30	56.349	-121.917	2.3	Calculated	1.9	ML
2016/03/29	01:13:08	55.068	-124.038	0.0	Fixed	1.8	ML
2016/03/28	06:12:27	56.922	-122.181	5.0	Fixed	1.8	ML
2016/03/27	19:31:45	56.281	-122.420	5.3	Calculated	1.0	ML
2016/03/23	22:15:34	56.955	-122.136	6.5	Calculated	2.0	ML
2016/03/23	02:34:53	56.312	-122.055	12.2	Calculated	2.0	ML
2016/03/22	21:32:43	55.103	-124.073	0.0	Fixed	2.0	ML
2016/03/22	02:20:09	57.283	-122.238	10.2	Calculated	1.5	ML
2016/03/21	00:13:25	56.292	-122.162	16.9	Calculated	0.5	ML
2016/03/20	09:19:31	56.299	-121.951	9.7	Calculated	1.8	ML

2016/03/19	09:32:12	56.293	-121.892	7.2	Calculated	1.1	ML
2016/03/19	06:02:07	56.349	-121.986	5.0	Fixed	1.9	ML
2016/03/19	05:28:23	56.279	-122.312	17.7	Calculated	1.2	ML
2016/03/19	00:14:01	56.948	-122.143	4.7	Calculated	2.2	ML
2016/03/19	00:13:00	56.314	-122.019	12.8	Calculated	1.8	ML
2016/03/17	14:08:00	57.272	-122.139	7.7	Calculated	2.4	ML
2016/03/16	21:33:08	55.104	-124.163	0.0	Fixed	2.0	ML
2016/03/16	05:05:50	57.296	-122.157	4.7	Calculated	1.8	ML
2016/03/16	02:42:34	56.305	-121.906	5.9	Calculated	1.8	ML
2016/03/16	01:45:03	56.332	-121.997	8.4	Calculated	2.0	ML
2016/03/15	20:55:18	56.274	-122.101	15.1	Calculated	1.6	ML
2016/03/15	09:37:07	56.313	-121.963	1.0	Fixed	2.2	ML
2016/03/14	16:38:37	57.306	-122.030	5.0	Fixed	2.1	ML
2016/03/12	08:09:04	56.342	-121.951	5.6	Calculated	2.2	ML
2016/03/11	19:31:25	56.943	-122.152	7.4	Calculated	1.9	ML
2016/03/11	13:56:32	56.972	-122.249	1.0	Fixed	2.3	ML
2016/03/11	07:43:34	56.316	-122.202	5.0	Fixed	1.0	ML
2016/03/10	12:35:15	56.996	-122.062	5.0	Fixed	2.2	ML
2016/03/10	02:37:13	56.965	-122.091	5.0	Fixed	3.1	ML
2016/03/09	17:09:14	56.254	-122.541	5.0	Fixed	2.1	ML
2016/03/09	04:38:05	56.318	-121.945	1.0	Fixed	2.2	ML
2016/03/08	08:28:59	56.947	-122.215	3.6	Calculated	1.9	ML
2016/03/08	07:09:49	56.680	-122.004	1.5	Calculated	1.9	ML
2016/03/07	22:30:01	55.066	-124.034	0.0	Fixed	2.5	ML
2016/03/07	15:00:02	56.961	-122.203	2.0	Calculated	2.0	ML

2016/03/07	01:06:17	56.953	-122.088	7.5	Calculated	2.3	ML
2016/03/04	17:41:00	56.963	-121.977	0.0	Fixed	2.4	ML
2016/03/04	03:02:49	56.482	-121.809	6.7	Calculated	2.3	ML
2016/03/03	21:08:47	56.776	-121.996	1.0	Fixed	1.9	ML
2016/03/03	07:43:25	57.047	-122.217	6.7	Calculated	2.4	ML
2016/03/02	20:21:32	56.981	-122.163	5.0	Fixed	1.8	ML
2016/03/01	21:46:00	56.971	-122.135	1.0	Fixed	1.9	ML
2016/03/01	16:28:17	56.942	-122.071	2.3	Calculated	1.9	ML
2016/03/01	16:27:37	56.480	-122.373	13.8	Calculated	1.9	ML
2016/03/01	14:59:19	56.959	-122.201	4.7	Calculated	1.9	ML
2016/03/01	13:22:00	56.342	-122.105	5.0	Fixed	1.7	ML
2016/02/29	19:38:17	55.114	-123.943	2.0	Calculated	2.3	ML
2016/02/27	23:34:41	55.138	-124.247	8.5	Calculated	2.2	ML
2016/02/27	18:23:17	56.299	-121.843	11.9	Calculated	2.0	ML
2016/02/27	13:03:08	56.596	-122.450	10.0	Fixed	2.3	ML
2016/02/27	03:16:14	56.791	-122.168	10.0	Fixed	2.3	ML
2016/02/26	19:36:14	56.515	-122.100	0.0	Fixed	2.2	ML
2016/02/26	19:21:00	56.885	-121.957	0.0	Fixed	2.1	ML
2016/02/25	03:31:24	57.014	-122.588	27.5	Calculated	2.2	ML
2016/02/24	09:18:10	57.051	-122.210	5.0	Fixed	2.1	ML
2016/02/23	18:39:20	56.477	-122.519	11.3	Calculated	1.9	ML
2016/02/22	22:40:17	55.020	-123.927	0.0	Fixed	1.8	ML
2016/02/22	18:44:51	56.493	-122.337	13.4	Calculated	2.0	ML
2016/02/22	14:40:38	57.076	-122.216	9.1	Calculated	2.0	ML
2016/02/22	10:24:38	56.502	-122.291	15.8	Calculated	2.3	ML

2016/02/22	05:43:43	56.539	-122.198	7.8	Calculated	2.4	ML
2016/02/22	03:28:43	57.038	-122.436	11.3	Calculated	2.2	ML
2016/02/22	02:16:25	56.494	-122.364	13.2	Calculated	2.2	ML
2016/02/22	00:57:49	56.479	-122.296	12.8	Calculated	1.8	ML
2016/02/22	00:49:25	56.481	-122.268	21.2	Calculated	2.0	ML
2016/02/21	09:51:28	57.045	-122.229	1.0	Fixed	3.0	ML
2016/02/20	23:58:35	55.095	-124.102	6.4	Calculated	2.5	ML
2016/02/20	21:12:55	56.212	-122.066	1.0	Fixed	2.0	ML
2016/02/19	21:00:51	57.291	-122.257	5.1	Calculated	2.3	ML
2016/02/19	14:24:50	57.290	-122.164	7.9	Calculated	2.1	ML
2016/02/19	11:35:51	57.277	-122.214	7.8	Calculated	1.7	ML
2016/02/19	11:15:08	57.276	-122.181	8.7	Calculated	2.6	ML
2016/02/19	11:13:22	57.278	-122.233	11.4	Calculated	1.9	ML
2016/02/19	08:08:09	57.282	-122.227	8.1	Calculated	1.8	ML
2016/02/17	04:26:09	56.057	-121.026	6.9	Calculated	1.8	ML
2016/02/17	03:17:44	56.691	-122.060	14.6	Calculated	1.9	ML
2016/02/16	20:47:04	57.051	-122.260	2.3	Calculated	2.3	ML
2016/02/16	19:10:43	56.950	-122.261	13.3	Calculated	1.8	ML
2016/02/15	18:45:18	55.058	-123.974	0.0	Fixed	2.1	ML
2016/02/15	17:19:25	56.809	-121.949	19.3	Calculated	1.7	ML
2016/02/13	18:43:53	55.108	-124.100	0.0	Fixed	2.3	ML
2016/02/12	21:00:41	57.239	-122.568	19.8	Calculated	1.7	ML
2016/02/11	18:04:50	57.291	-122.202	4.9	Calculated	2.0	ML
2016/02/11	17:56:53	57.276	-122.212	7.2	Calculated	2.8	ML
2016/02/11	17:49:12	57.288	-122.211	5.7	Calculated	1.7	ML

2016/02/11	17:42:17	57.291	-122.222	4.0	Calculated	1.9	ML
2016/02/10	04:14:49	56.224	-122.100	1.0	Fixed	2.1	ML
2016/02/10	02:39:07	56.200	-122.224	7.5	Calculated	2.2	ML
2016/02/09	22:20:45	56.211	-122.179	1.0	Fixed	1.8	ML
2016/02/09	17:50:53	56.155	-122.392	1.0	Fixed	2.3	ML
2016/02/09	03:44:58	56.131	-122.368	12.2	Calculated	2.0	ML
2016/02/08	21:10:30	56.162	-122.268	7.6	Calculated	2.5	ML
2016/02/08	18:34:11	56.195	-122.248	10.0	Calculated	2.5	ML
2016/02/08	02:32:34	56.135	-122.319	16.9	Calculated	2.0	ML
2016/02/08	01:59:24	56.212	-122.238	7.6	Calculated	2.3	ML
2016/02/07	23:05:04	55.129	-124.125	0.0	Fixed	2.2	ML
2016/02/07	07:55:57	57.046	-122.292	8.6	Calculated	2.3	ML
2016/02/06	11:41:13	57.041	-122.272	1.0	Fixed	2.1	ML
2016/02/05	23:00:51	55.145	-124.101	0.0	Fixed	3.1	ML
2016/02/01	22:38:25	55.035	-123.938	0.0	Fixed	2.1	ML
2016/01/29	22:31:06	55.004	-123.836	5.6	Calculated	2.3	ML
2016/01/23	22:36:16	55.111	-124.074	5.0	Fixed	2.7	ML
2016/01/13	23:19:17	55.095	-124.071	0.0	Fixed	2.3	ML
2016/01/13	02:17:45	56.611	-121.778	10.0	Fixed	1.9	ML
2016/01/11	05:52:09	57.041	-122.238	9.1	Calculated	2.5	ML
2016/01/11	00:24:54	56.409	-121.804	20.0	Fixed	2.0	ML
2016/01/10	18:42:57	55.074	-124.037	0.0	Fixed	2.5	ML
2016/01/10	14:54:48	56.245	-122.228	1.0	Fixed	2.2	ML
2016/01/09	10:03:09	56.941	-122.162	1.0	Fixed	1.8	ML
2016/01/08	18:56:51	55.079	-123.948	11.9	Calculated	2.2	ML

2016/01/07	18:32:05	55.142	-124.271	1.0	Fixed	1.8	ML
2016/01/06	19:30:37	56.108	-122.163	20.0	Fixed	1.6	ML
2016/01/06	17:45:26	56.183	-122.237	1.0	Fixed	1.7	ML
2016/01/06	00:22:58	55.075	-124.062	0.0	Fixed	2.2	ML
2016/01/04	12:27:10	56.204	-122.083	10.0	Fixed	2.0	ML
2016/01/04	11:28:15	56.193	-122.090	5.0	Fixed	2.0	ML
2016/01/01	18:06:26	56.491	-122.344	1.0	Fixed	1.9	ML
2016/01/01	17:01:46	56.505	-122.429	1.0	Fixed	2.0	ML
2016/01/01	12:05:42	56.306	-121.878	1.0	Fixed	2.0	ML
2016/01/01	00:37:53	56.434	-121.861	16.0	Calculated	2.5	ML

Appendix B: Yukon Geological Survey Performance Report

Figure B1 shows the distribution of the stations in the Liard Basin and surrounding areas. The red triangles are the new stations deployed by the Yukon Geological Survey (YGS) and the BC Seismic Research Consortium in 2016. The YGS provided instruments for four of the stations (TOAD, LIRD, BEAV, KOTA) while NRCan acquired instruments for the fifth station (NAHA). The black triangles represent stations that have been operating since 1999 (FNBB), and 2013 (NBC1, NBC2, NBC3, NBC6, FLDN, WTLY, and TGTN). All seismographic stations are equipped with broadband sensors and send real-time waveforms to the Pacific Geoscience Center in Sidney, BC and Incorporated Research Institutions for Seismology data center in Seattle, Washington.

Also shown in Figure B1 is the seismic activity since 1985 to October 2017 from NRCan earthquake catalogue with magnitude range 0.9-5.3 (blue dots). Different magnitude scales were reported for these events with the majority of earthquakes having local magnitude scale (M_L). Other magnitude scales include the Nuttli scale (M_N), moment magnitude (M_w) and body-wave magnitude (M_B). Figure B2a shows the occurrence of the earthquakes shown in Figure B1 versus year. Dashed lines show the installation year of the seismographic stations. Figure B2b shows the number of events in each magnitude bin.

I followed the methodology described in Babaie Mahani et al. (2016) to evaluate the performance of seismographic stations in the area by calculating the minimum detectable magnitude. A 100 by 100 grid was first generated for the study area. By placing seismic sources of variable magnitudes (0-4 with 0.2 increments) at each grid point, ground motion amplitudes (PGV) were estimated at the location of each seismographic stations. For

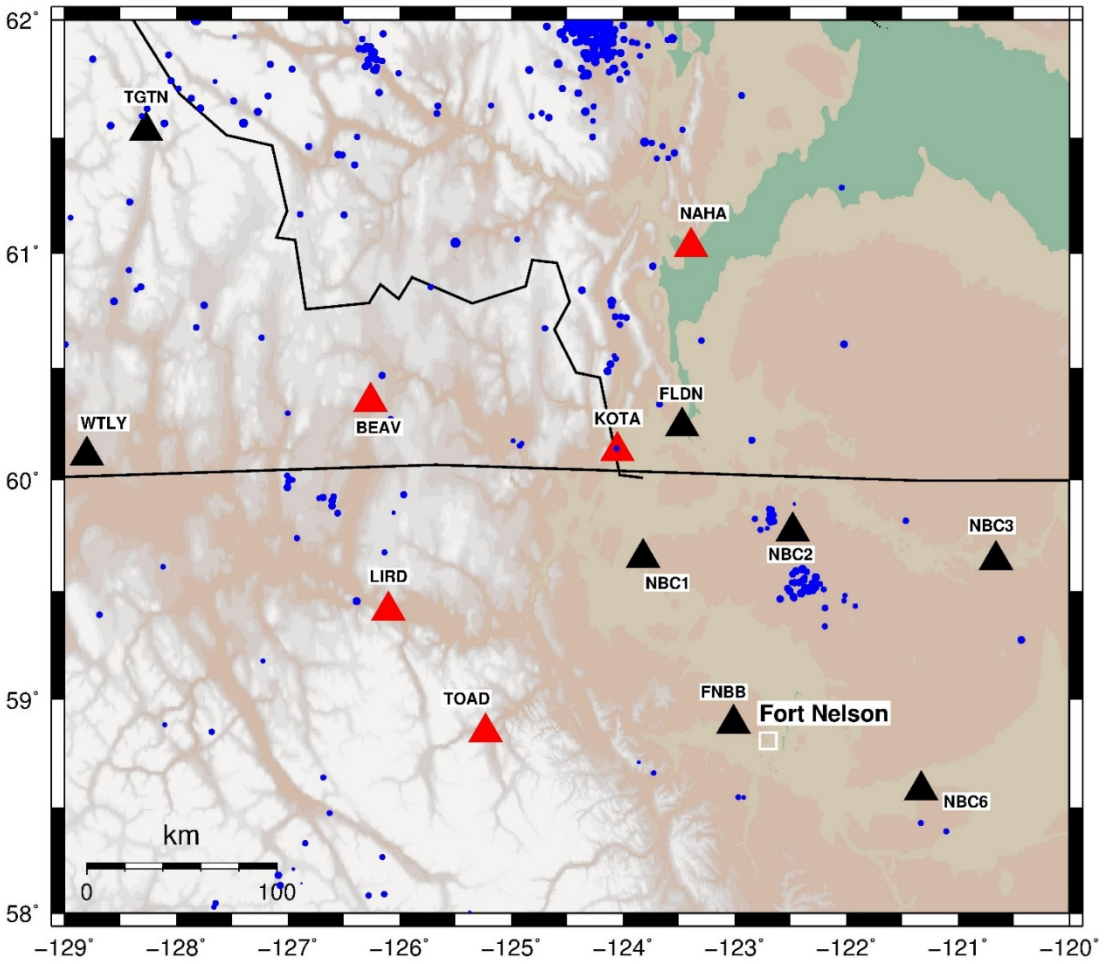

Figure B1. Broadband seismographic stations in the Liard Basin and surrounding areas. Red triangles are the new stations deployed in 2016. Black triangles are the stations deployed before then. Blue dots are the events between 1985 and 2017 from Natural Resources Canada earthquake catalogue.

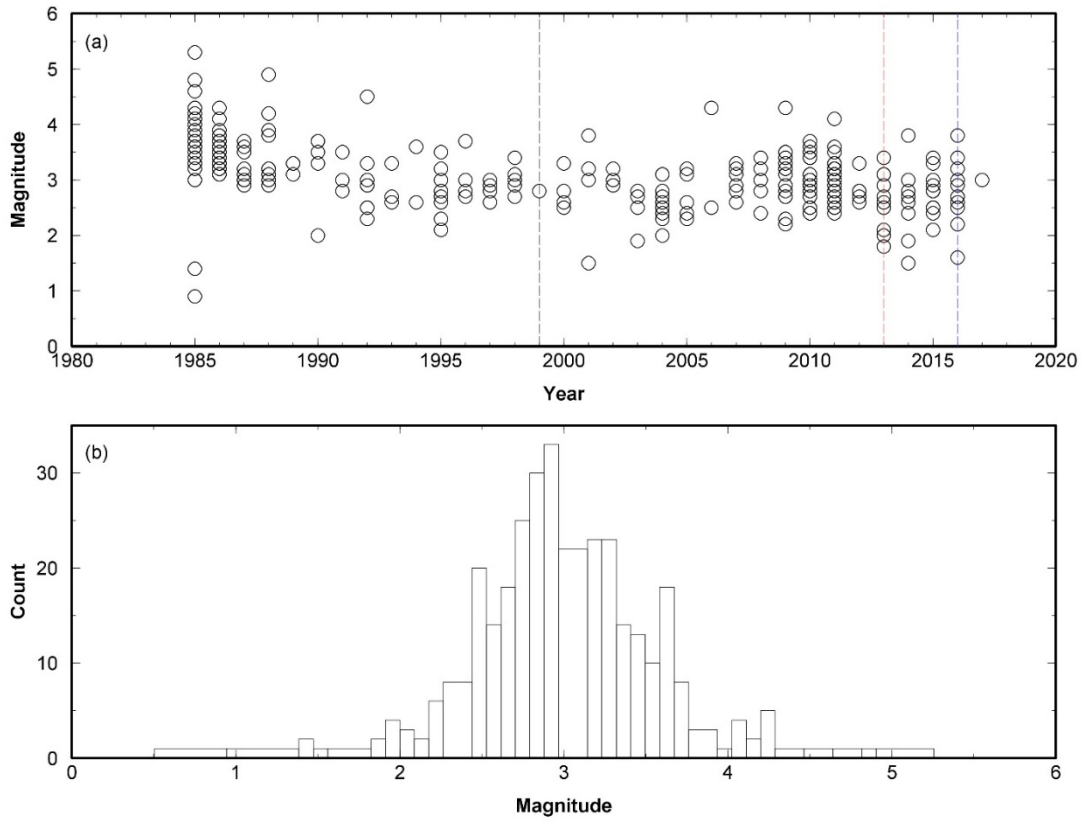

Figure B2. (a) temporal distribution of seismic activity shown in Figure B1. Vertical dashed lines indicate the installation year of the seismographic stations. (b) frequency-magnitude distribution of the events.

each grid point-station pair, I then calculated the ratio of PGV to the average background noise for all magnitudes. The source signal at any given station was considered identifiable if the signal-to-noise ratio (SNR) exceeds 10. The choice of SNR $\geq$ 10 was to ensure unambiguous identification of earthquake signals at each station. An event is considered locatable if at least four stations have identifiable signals (i.e., SNR $\geq$ 10). Based on these criteria, the variability of minimum detectable magnitude of regional earthquakes in the study area was mapped and the results are shown in Figure B3. The minimum detectable magnitude can be considered as the theoretical threshold for any seismic event to be located by the regional seismograph network (Babaie Mahani et al., 2016).

The minimum detectable magnitude ranges between 1.2 in the well-covered regions and increases to 2.2 outside of the network (Figure B3). The uncertainty in the location of an event is usually shown by error ellipses which represent the shape and orientation of the error axes (semi-major and semi-minor axes of the error ellipse). Here, the square root of the sum of semi-major and semi-minor error axes were used to calculate the uncertainty and it is shown in Figure B4 for events with magnitude 2.5. The total epicentral uncertainty in areas well covered by the seismographic stations is below 2 km and increases to the edge of the network. The red ellipses show the shape and orientation of the error axes in some locations which depend on the geometry of the seismographic network.

Although there has not been much seismic activity in the Liard Basin, the existence of the new seismographic stations (red triangles in Figure B1) help with establishing detailed base-line analysis for the background seismicity in the area prior to the foreseeable increase in oil and gas activities and induced seismicity.

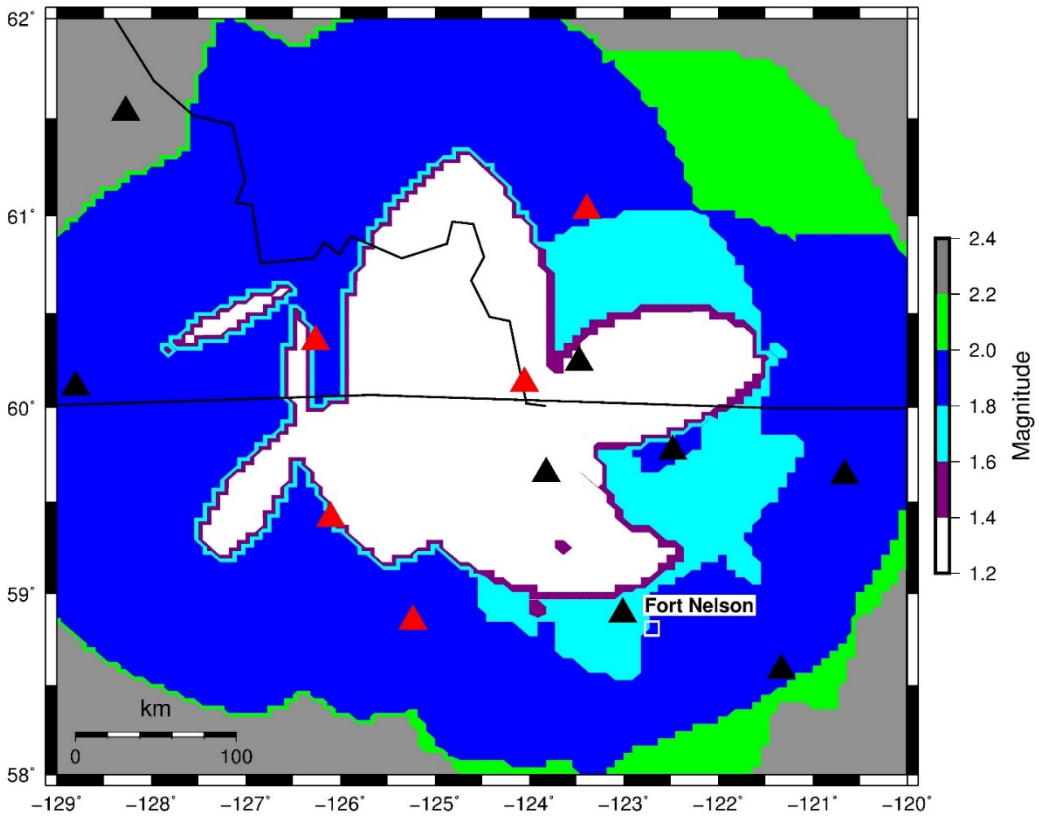

Figure B3. Minimum detectable magnitude in the Liard Basin and surrounding areas. Red triangles are the new stations deployed in 2016. Black triangles are the stations deployed before then.

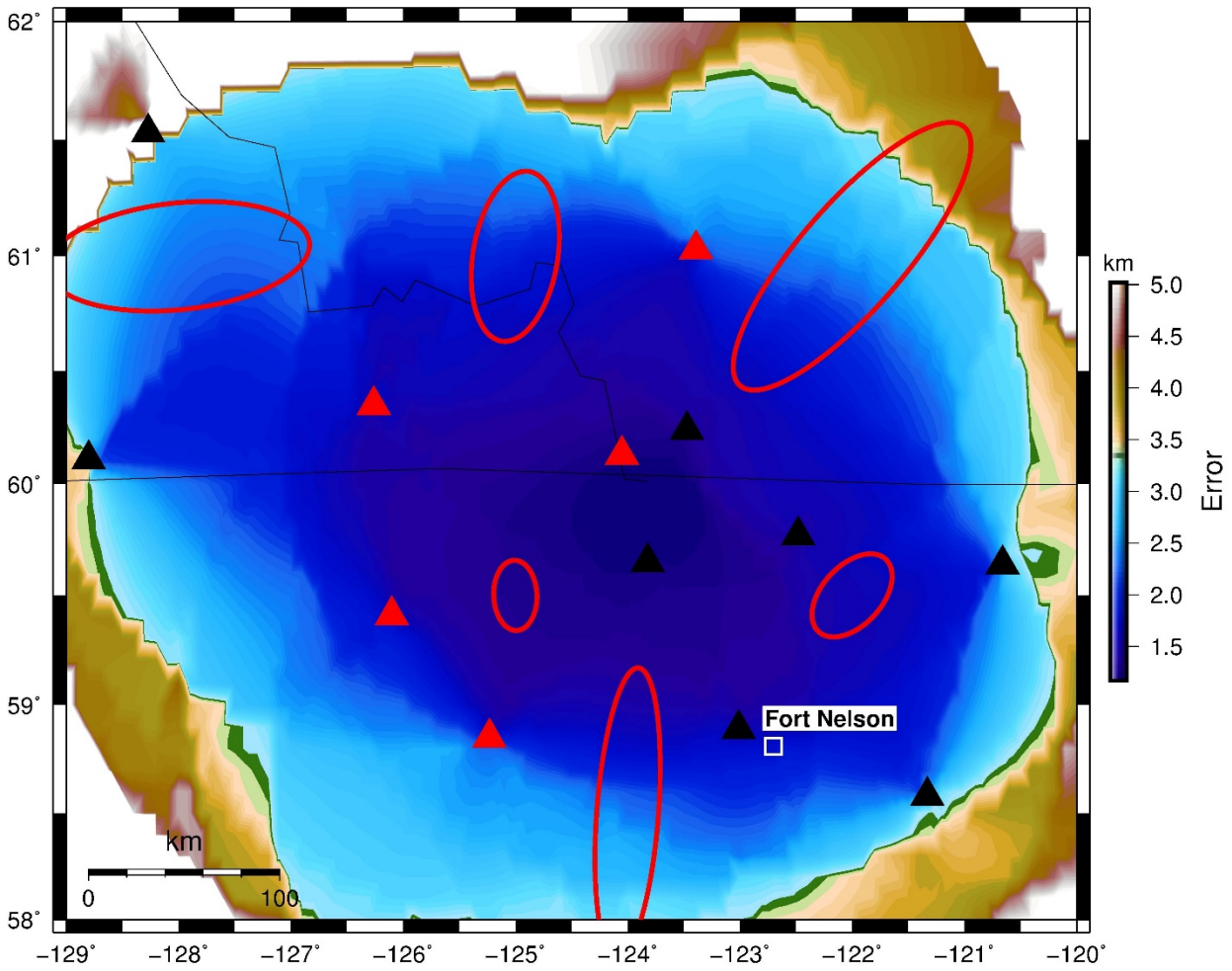

Figure B4. Total uncertainty in the epicentral location for events with magnitude 2.5. The ellipses show the orientation and shape of the error axes at some locations. Red triangles are the new stations deployed in 2016. Black triangles are the stations deployed before then.